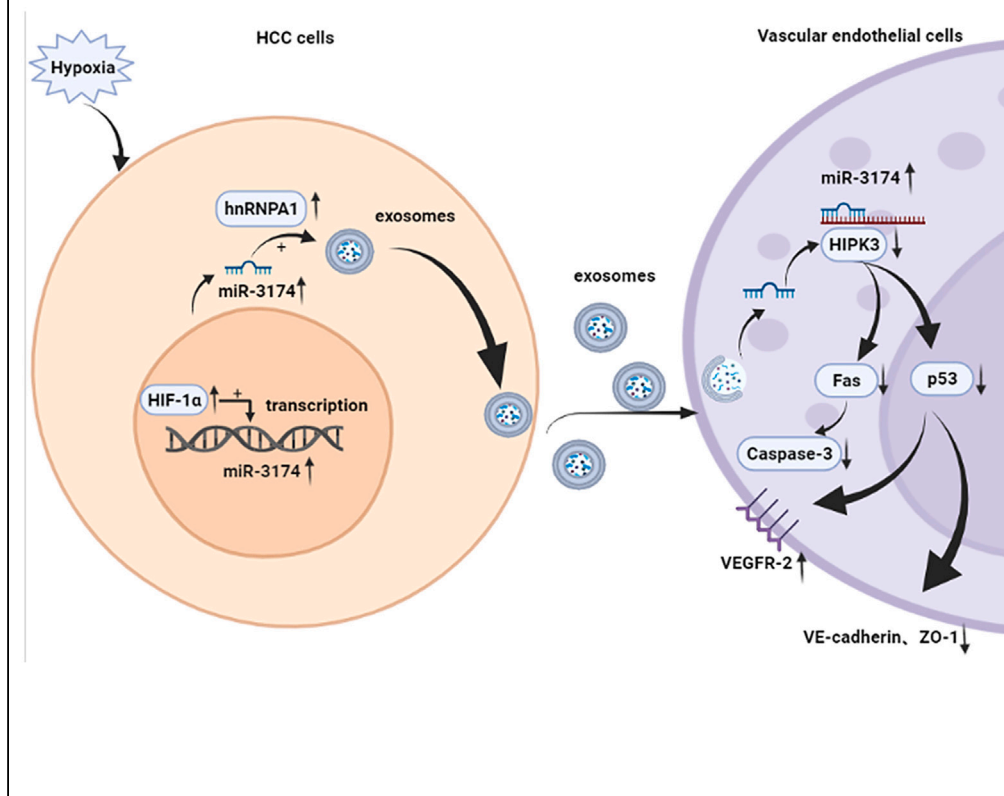


Article

Exosomal miR-3174 induced by hypoxia promotes angiogenesis and metastasis of hepatocellular carcinoma by inhibiting HIPK3

1. The image's components have been organized to tell the story from left to right.
2. The colors and boxes have been adjusted to highlight and direct focus toward the most relevant information.



Xiao Yang, Mingyu Wu, Xiangxu Kong, ..., Lianbao Kong, Fei Qiu, Wangjie Jiang

lbkong@njmu.edu.cn (L.K.)
qiufeiie@126.com (F.Q.)
drjiang@njmu.edu.cn (W.J.)

Highlights

MiR-3174 can be unidirectionally transmitted to HUVECs through exosomes

Exosomal miR-3174 promotes angiogenesis and metastasis of HCC by inhibiting HIPK3

Under hypoxia, HIF-1α promotes transcription of miR-3174 in HCC cells

Under hypoxia, HNRNPA1 promotes the assembly of miR-3174 into HCC-derived exosomes

Yang et al., iScience 27, 108955
February 16, 2024 © 2024 The Author(s).
<https://doi.org/10.1016/j.isci.2024.108955>



Article

Exosomal miR-3174 induced by hypoxia promotes angiogenesis and metastasis of hepatocellular carcinoma by inhibiting HIPK3

Xiao Yang,^{1,3,6} Mingyu Wu,^{1,6} Xiangxu Kong,^{3,6} Yun Wang,⁴ Chunyang Hu,³ Deming Zhu,² Lianbao Kong,^{2,3,*} Fei Qiu,^{5,*} and Wangjie Jiang^{2,3,7,*}

SUMMARY

Hepatocellular carcinoma (HCC) is a highly malignant tumor with rich blood supply. HCC-derived exosomes containing hereditary substances including microRNAs (miRNAs) were involved in regulating tumor angiogenesis and metastasis. Subsequently, series experiments were performed to evaluate the effect of exosomal miR-3174 on HCC angiogenesis and metastasis. HCC-derived exosomal miR-3174 was ingested by human umbilical vein endothelial cells (HUVECs) in which HIPK3 was targeted and silenced, causing subsequent inhibition of Fas and p53 signaling pathways. Furthermore, exosomal miR-3174 induced permeability and angiogenesis of HUVECs to enhance HCC progression and metastasis. Under hypoxia, upregulated HIF-1 α further promoted the transcription of miR-3174. Moreover, HNRNPA1 augmented the package of miR-3174 into exosomes. Clinical data analysis confirmed that HCC patients with high-level miR-3174 were correlated with worse prognosis. Thus, exosomal miR-3174 induced by hypoxia promotes angiogenesis and metastasis of HCC by inhibiting HIPK3/p53 and HIPK3/Fas signaling pathways. Our findings might provide potential targets for anti-tumor therapy.

INTRODUCTION

Hepatocellular carcinoma (HCC) is one of the most malignant tumors with high incidence and poor prognosis worldwide.¹ Surgical resection is one of the most effective options for HCC; however, high mortality and recurrence after surgery remain giant threat for patients. In addition, many patients in advanced stage lose the opportunity for surgery. In recent decades, anti-angiogenic targeted therapies such as sorafenib-based regimens have brought a breakthrough in the treatment of advanced and recurrent HCC. Even that, tumor-induced neovascularization limits the sustained efficacy of the therapy. Moreover, neovascularization increases the metastatic potential of cancer cells to other organs. Therefore, new breakthrough need be probed to break this bottleneck.

Being the smallest extracellular vesicles (30–200 nm) with a double-layer membrane, exosomes can be secreted by tumor cells, immune cells, and other living cells and widely distributed in blood, urine, and other body fluids.² As the vehicle mediating information exchange and cellular physiological functions, exosomes carry genetic cargoes (DNA, RNA, and proteins) and transfer them to target cells through membrane fusion or endocytosis.³ Published studies have reported that tumor-derived exosomes (TEXs) are more abundant and widely involve in TME reprogramming. For instance, TEXs mediate the information transferring of tumor cells to mesenchymal cells including vascular endothelial cells (VECs), which then in turn affect the malignant behaviors of tumor cells.⁴ For example, Shephard et al.⁵ revealed that exosomal message RNAs (mRNAs) could be effective biomarkers for monitoring TME remodeling. Tumor-derived exosomal proteins such as THBS1 regulate polarization of macrophages.⁶ Our previous study has revealed that miR-3174 facilitates HCC progression relied on FOXO1; however, whether miR-3174 in HCC involves in the TME regulation in exosome-dependent manner remains to be elucidated.

MiRNAs are members of small noncoding RNA family, and they are mainly involved in posttranscriptional regulation.¹ Extensive studies have reported that exosomal miRNAs, the most highly enriched content in exosomes, regulate tumor progression and TME remodeling.^{1,3,7,8} For example, exosomal miR-1247-3p secreted by HCC activates cancer-associated fibroblasts (CAFs) to induce lung metastasis of HCC.⁹

¹Department of Hepatobiliary Surgery, The Affiliated Wuxi People's Hospital of Nanjing Medical University, Wuxi People's Hospital, Wuxi Medical Center, Nanjing Medical University, 299 Qingyang Road, Wuxi, Jiangsu 214023, China

²Hepatobiliary Center, The First Affiliated Hospital of Nanjing Medical University, Nanjing, Jiangsu 210000, China

³Key Laboratory of Liver Transplantation, Chinese Academy of Medical Sciences, NHC Key Laboratory of Living Donor Liver Transplantation (Nanjing Medical University), Nanjing, Jiangsu 210000, China

⁴Department of Hepatobiliary Surgery, Xuzhou City Central Hospital, The Affiliated Hospital of the Southeast University Medical School (Xu zhou), The Tumor Research Institute of the Southeast University (Xu zhou), Xuzhou clinical college of Xuzhou Medical University, 199 Jiefang South Road, Xuzhou, Jiangsu 221009, China

⁵Department of Anesthesiology, The Second Hospital of Nanjing, Nanjing, Jiangsu 210000, China

⁶These authors contributed equally

⁷Lead contact

*Correspondence: lbkong@njmu.edu.cn (L.K.), qjufeie@126.com (F.Q.), drjiang@njmu.edu.cn (W.J.)
<https://doi.org/10.1016/j.isci.2024.108955>



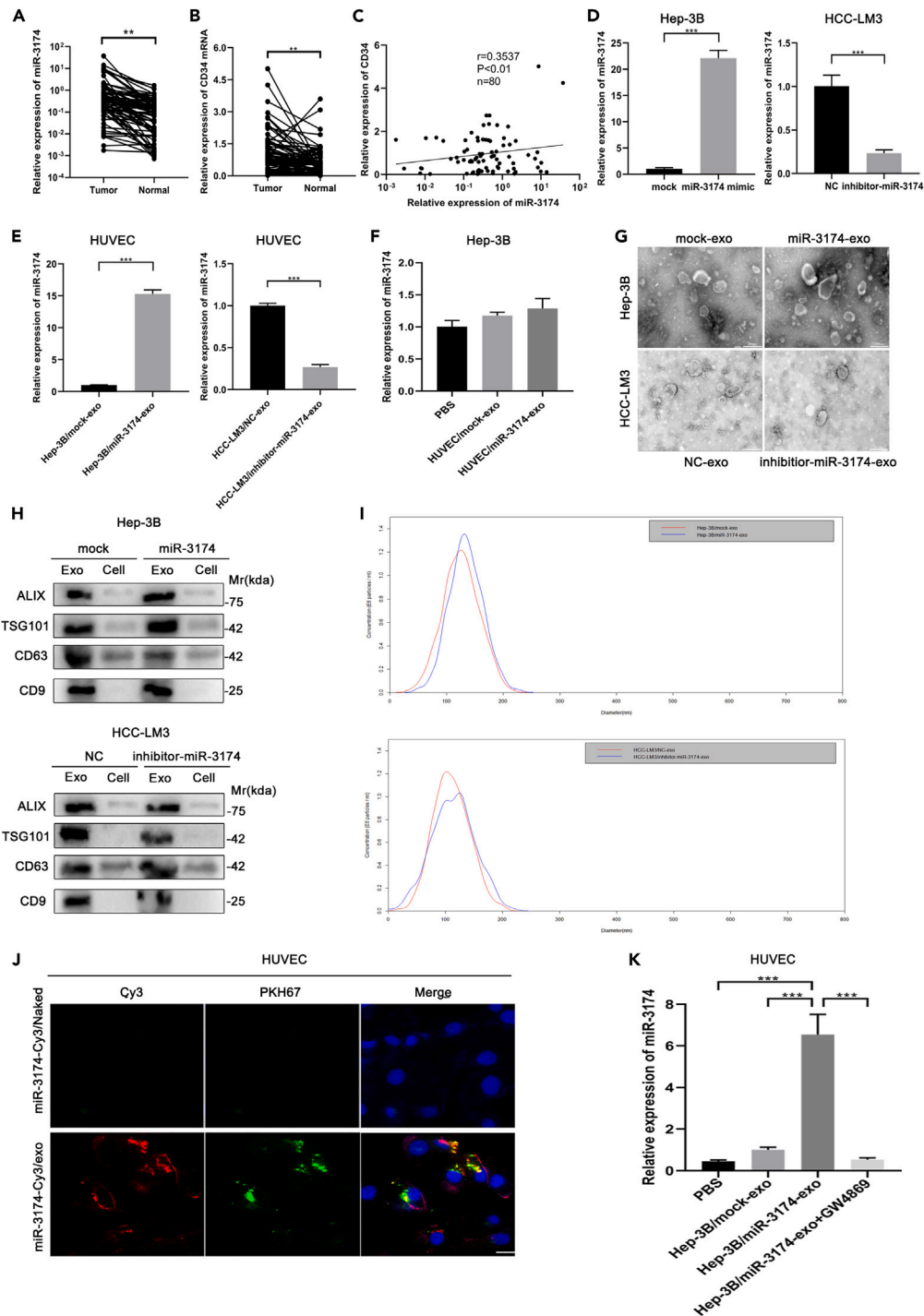


Figure 1. Exosomal miR-3174 secreted by HCC cells can be transmitted to HUVECs

(A and B) QRT-PCR analysis of miR-3174 and CD34 expression levels in HCC tissues and adjacent normal liver tissues (n = 80).

(C) Pearson's correlation analysis of expression levels of miR-3174 and CD34 in HCC tissues (n = 80). Pearson's correlation coefficient (r) and p value are shown in the chart. p value is from Pearson's test.

(D) RT-qPCR analysis of expression levels of miR-3174 in Hep-3B cells (transfected with mimic-NC or miR-3174 mimics) and HCC-LM3 cells (transfected with inhibitor-NC or inhibitor-miR-3174).

(E) RT-qPCR analysis of miR-3174 expression levels in HUVECs cocultured with exosomes secreted by Hep-3B/mock, Hep-3B/miR-3174, HCC-LM3/NC-, and HCC-LM3/inhibitor-miR-3174 cells.

Figure 1. Continued

- (F) RT-qPCR analysis of miR-3174 expression levels in Hep-3B cells incubated with PBS and exosomes derived from HUVECs transfected with mimic-NC (HUVEC/mock-exo) or miR-3174 mimics (HUVEC/miR-3174-exo).
- (G) Electron micrographs of exosomes derived from cells in four groups: Hep-3B/mock, Hep-3B/miR-3174, HCC-LM3/NC, and HCC-LM3/inhibitor-miR-3174. Scale bar represents 200 nm.
- (H) Western blot analysis of expression levels of exosome markers (ALIX, TSG101, CD63, and CD9) in cells and their derived exosomes in abovementioned four groups.
- (I) NTA analysis of the abundance of exosomes in abovementioned four groups.
- (J) (Top panels) HUVECs incubated with naked-miR-3174-Cy3 were used as a negative control. (Bottom panels) Exosomal miR-3174 labeled with Cy3 (red) and PKH67 (green) in HUVECs (DAPI) were observed after incubated with Hep-3B/miR-3174-exo for 24 h. Scale bar represents 25 μ m.
- (K) RT-qPCR analysis of miR-3174 expression levels in HUVECs incubated with PBS, Hep-3B/mock-exo, Hep-3B/miR-3174-exo, and Hep-3B/miR-3174-exo+GW4869 for 24 h. Error bars represent mean \pm SEM of three replicates (n = 3). (*p < 0.05, **p < 0.01, ***p < 0.001).

Furthermore, miR-M2 macrophages-derived exosomal miR-23a-3p was reported to enhance the vascular permeability to promote HCC metastasis.¹⁰ It was clear that exosomal miRNAs act as a bridge between cell-to-cell communication.

More than that, variety of potential of hydrogen (pH), hypoxia, and other conditions can also affect the secretion of exosomal miRNAs. It has been reported that hypoxia can promote the production of exosomal miR-27-3b in cardiac microvascular endothelial cells.¹¹ However, the concrete mechanisms of exosomal miRNAs remained unclear. In our previous study, we identified that upregulated miR-3174 can promote HCC growth.¹² On this basis, we conducted a more in-depth study. Herein, we focused on the effects of HCC-derived exosomal miR-3174 induced by hypoxia on angiogenesis and metastasis of HCC. We investigated whether HCC-derived exosomal miR-3174 could be transmitted to human umbilical vein endothelial cells (HUVECs) and its role in inducing angiogenesis and metastasis of HCC.

RESULTS**HCC cells deliver exosomal miR-3174 to HUVECs**

Based on pan-cancer analysis in TCGA database, we found that miR-3174 was highly expressed in multiple range of cancers including HCC (Figures S1A and S1B). Our previous study has shown that miR-3174 acts as a critical role in facilitating HCC progression.¹² Further analysis of RT-qPCR data of 80 pairs of HCC samples showed that CD34 (the biomarker of VECs) were both highly expressed and positively correlated with miR-3174 level in HCC tissues significantly (Figures 1A–1C), prompting us to speculate that miR-3174 might be associated with the increased vascular components in HCC tissue. To verify the speculation, HUVECs were separately cocultured with PBS or exosomes derived from QSG-7701, Hep-3B, and HCC-LM3 cells for 48 h. Subsequent RT-qPCR analysis showed that miR-3174 was upregulated in HUVECs with Hep-3B/exo and HCC-LM3/exo incubation. Conversely, little increased expression of miR-3174 was detected in HUVECs cocultured with exosomes from normal hepatocytes (QSG-7701) (Figure S1C). Then, we constructed miR-3174 overexpression (miR-3174 mimics) or knockdown (inhibitor-miR-3174) cell lines in HCC-LM3 or Hep-3B cells, respectively. The transfection efficiency was confirmed (Figure 1D). Similarly, under the treatment of exosomes derived from Hep-3B transfected with miR-3174 mimics for 48 h, the level of miR-3174 in HUVECs was upregulated. However, the opposite result was observed in HUVECs incubated with the exosomes released from miR-3174-silencing Hep-3B cells (Figure 1E). We thus assumed that miR-3174 could be delivered from HCC cells to HUVECs via exosomes. To exclude the effect of HUVECs-derived miR-3174 on HCC cells, we cocultured Hep-3B cells with exosomes secreted from miR-3174-transfected HUVECs. Little alteration of the miR-3174 expression level in Hep-3B cells was observed (Figure 1F). These vesicles isolated from Hep-3B and HCC-LM3 cells were detected by transmission electron microscopy and verified less than 200 nm in diameter (Figure 1G). Further analysis showed that the expression levels of ALIX, TSG101, CD63, and CD9 were highly expressed in isolated vesicles rather than in Hep-3B and HCC-LM3 cells (Figure 1H). In addition, Nanoparticle Tracking Analysis (NTA) also proved that the diameters of Hep-3B- and HCC-LM3-cell-derived exosomes were distributed at 30–200 nm (Figure 1I), which further confirmed the vesicles as purified exosomes. To simulate the transmission process, we labeled miR-3174 mimics and exosomes with Cy3 (red) and PKH67 separately. After coculturing HUVECs with Hep-3B-cell-derived exosomes, the merged signal of Cy3 and PKH67 was observed, hinting that exosomal miR-3174 could be transported to HUVECs (Figure 1J). Subsequent RT-qPCR analysis confirmed that miR-3174 in HUVECs treated with Hep-3B/miR-3174-exo for 24 h was higher expressed than that in other groups, which can be inhibited by GW4869 (Figure 1K). These experimental results exhibited that exosomal miR-3174 was uniaxially delivered from HCC cells to HUVECs and increased the expression level of miR-3174 in HUVECs.

HCC-derived exosomal miR-3174 promotes angiogenesis of HUVECs and increases their permeability *in vitro*

To explore the effects of exosomal miR-3174 on HUVECs, we loaded miR-3174 mimics and miR-3174 inhibitor into the exosomes released from Hep-3B (Hep-3B/miR-3174-exo) and HCC-LM3 cells (HCC-LM3/inhibitor-miR-3174-exo) separately for subsequent experiments. Scratch healing assay and transwell migration assay showed that Hep-3B/miR-3174-exo significantly improved the migration of HUVECs, whereas HCC-LM3/inhibitor-miR-3174-exo markedly reduced their motilities (Figures 2A–2D). Tube formation assay and 3D spheroid sprouting assay confirmed that HUVECs cocultured with Hep-3B/miR-3174-exo possessed formidable angiogenesis ability compared with control group (Hep-3B/mock-exo). However, the angiogenesis of HUVECs incubated with HCC-LM3/inhibitor-miR-3174-exo was restrained (Figures 2E–2H). *In vitro* vascular permeability assay showed that Hep-3B/miR-3174-exo increased the leakiness of HUVECs, whereas the opposite result was detected in HCC-LM3/inhibitor-miR-3174-exo group (Figures 2I and 2J). These data showed that HCC-derived exosomal miR-3174 promoted angiogenesis of HUVECs and increased the permeability.

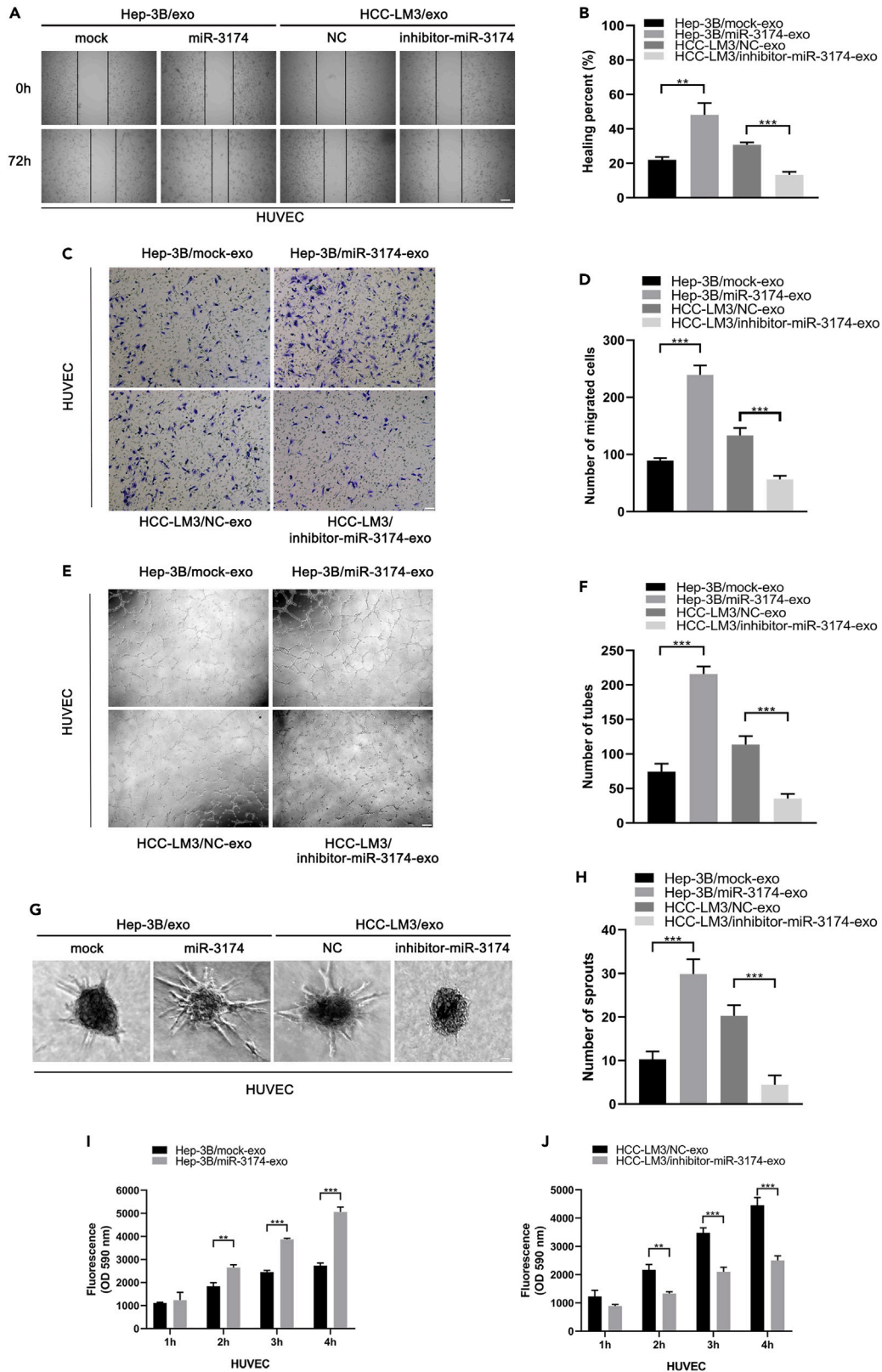


Figure 2. Exosomal miR-3174 promotes angiogenesis and enhances permeability of HUVECs *in vitro*

(A and B) The percentage of healing area of HUVECs incubated with exosomes secreted by cells in four groups: Hep-3B/mock, Hep-3B/miR-3174, HCC-LM3/NC, and HCC-LM3/inhibitor-miR-3174 for 72 h in scratch healing assay. Scale bar represents 100 μ m.

(C and D) The numbers of migrated HUVECs incubated with exosomes secreted by cells in abovementioned four groups in transwell migration assay. Scale bar represents 100 μ m.

(E and F) The numbers of tubes formed by HUVECs incubated with exosomes secreted by cells in abovementioned four groups in tube formation assay. Scale bar represents 100 μ m.

(G and H) The numbers of sprouts formed by HUVEC spheroids cocultured with exosomes secreted by cells in abovementioned four groups for 48 h in 3D spheroid sprouting assay. Scale bar represents 50 μ m.

(I and J) Fluorescence intensities at OD 590 nm of the HUVECs treated with Rhodamine B isothiocyanate-dextran (70 kDa) detected at 1, 2, 3, and 4 h after exposure to exosomes derived from cells in abovementioned four groups for 72 h. Error bars represent mean \pm SEM of three replicates (n = 3). (*p < 0.05, **p < 0.01, ***p < 0.001).

Exosomal miR-3174 promotes HCC progression and metastasis by inducing angiogenesis and enhancing vascular permeability *in vivo*

Based on the *in vitro* results, we focused on whether exosomal miR-3174 promoted HCC progression and metastasis by regulating angiogenesis and vascular permeability *in vivo*. Aortic ring assay revealed that Hep-3B/miR-3174-exo enhanced the budding ability of aortas, whereas HCC-LM3/inhibitor-miR-3174-exo inhibited sprouts of aortas substantially (Figures 3A and 3B). Then subcutaneous transplanted tumor models of Hep-3B cells in nude mice were constructed, and the photograph of these tumors in Hep-3B/mock-exo and Hep-3B/miR-3174-exo was also provided (Figure 3C). By measuring the volumes and weights of these transplanted tumors, we realized that exosomal miR-3174 accelerated growth of tumors in Hep-3B/miR-3174-exo group (Figures 3D and 3E). Similarly, RT-qPCR analysis showed that miR-3174 was higher expressed in Hep-3B/miR-3174-exo group than that in Hep-3B/mock-exo group (Figure 3F). Immunohistochemical staining analysis showed that the expression levels of Ki67 and CD34 were increased significantly in Hep-3B/miR-3174-exo group, suggesting that exosomal miR-3174 might promote HCC progression by increasing the vascular density of tumor tissues (Figure 3G). Immunofluorescence staining showed that the fluorescence intensity of rhodamine B (red) in Hep-3B/miR-3174-exo treatment group was significantly enhanced compared with that in control group (Figures 3H and 3I). The above findings indicated that neovascularizations induced by exosomal miR-3174 were more hypertonic compared with normal blood vessels. As before, we found more metastatic lesions in lung tissues of mice treated with Hep-3B/miR-3174-exo, and the fluorescence intensity of Rhodamine B (red) was markedly enhanced (Figures 3J–3M). However, the fluorescence intensity of Rhodamine B was impaired after treating with HCC-LM3/inhibitor-miR-3174-exo (Figures 3L and 3M). Therefore, exosomal miR-3174 promoted HCC progression and metastasis by inducing angiogenesis and enhancing vascular permeability *in vivo*.

Exosomal miR-3174 promotes angiogenesis and enhances vascular permeability by targeted inhibition of HIPK3

To explore the target genes of exosomal miR-3174 in HUVECs, we probed the potential target genes of miR-3174 in four public databases (TargetScan, miRWalk, miRDB, and miRPathDB). Totally, 47 genes were selected as potential target of miR-3174 by Venn diagram and database retrieval (Figure 4A). To find the genes specifically expressed in HUVECs, we explored the single-cell database PanglaoDB and found that homeodomain-interacting protein kinase 3 (HIPK3) was mainly expressed in endothelial cells (ECs) and fibroblasts (Figure S2A). Pearson's correlation analysis of HIPK3 expression levels and the abundances of interstitial cells in HCC tissues based on TCGA-LIHC database confirmed that HIPK3 was remarkably associated with the abundance of ECs (r = 0.61) (Figure S2B). Moreover, we found HIPK3 was also mainly enriched in three types of cells in liver including VECs based on HPA database exploration (Figure S2C). HIPK3 was thus identified as potential target of miR-3174 in HUVECs. Pan-cancer analysis of HIPK3 in Tumor database confirmed that HIPK3 was low-expressed in cancer tissues including HCC (Figure S2D). Consistently, the expression levels of HIPK3 in HCC cell lines (Hep-3B, HCC-LM3) was lower than that in hepatocytes (QSG-7701) (Figure S2E). Survival analysis via Kaplan-Meier Plotter database also showed that low expression level of HIPK3 meant shorter overall survival (OS), relapse-free survival (RFS), and disease-specific survival (DSS) of HCC patients (Figures S2F–S2H). Western blot analysis of three pairs of tissues confirmed that HIPK3 was lower expressed in HCC than that in adjacent tissues (Figure S2I). Similarly, RT-qPCR analysis also indicated that HIPK3 was highly expressed in adjacent liver tissues than that in HCC tissues (n = 80) (Figure 4B). Pearson's correlation analysis showed that the expression level of HIPK3 was negatively correlated with miR-3174 in HCC samples (n = 80) (Figure 4C). Subsequently, we obtained the predicted binding sites of 3'-UTR region of HIPK3 and miR-3174 from TargetScan database, which were then mutated (Figure 4D). Confirmed by dual luciferase report experiment, the luciferase activity in HEK293T cells transfected with HIPK3-WT-3'UTR plasmids was abated significantly in the presence of miR-3174 mimics. However, little change in other groups was detected (Figure 4E). Therefore, HIPK3 might be targeted and silenced by miR-3174.

HIPK family acts as transcriptional coregulators involved in various cellular biological activities.¹³ We suspected that exosomal miR-3174-mediated vascular permeability and angiogenesis of HUVECs relied on HIPK3 and its downstream signaling pathway. We performed Gene Ontology (GO) enrichment analysis on miR-3174 (Threshold, p value < 0.05) and predicted the proteins that can interact with HIPK3 in STRING database. We noticed that both miR-3174 and HIPK3 might be associated with p53 signaling pathway (Figures S1D and 4F). Similarly, according to the correlation analysis and single-sample gene set enrichment analysis (ssGSEA) based on TCGA-LIHC database, the expression level of HIPK3 was positively correlated with the expression level of TP53 and the activation of p53 signaling pathway in HCC (Figures 4G and 4H). Then, we simulated the binding of HIPK3 and p53 protein by molecular docking on HSYMDOCK server, and the model was shown in the chart (confidence score = 0.93) (Figure 4I). To verify the binding of HIPK3 and p53, immunofluorescence was performed and confirmed that HIPK3

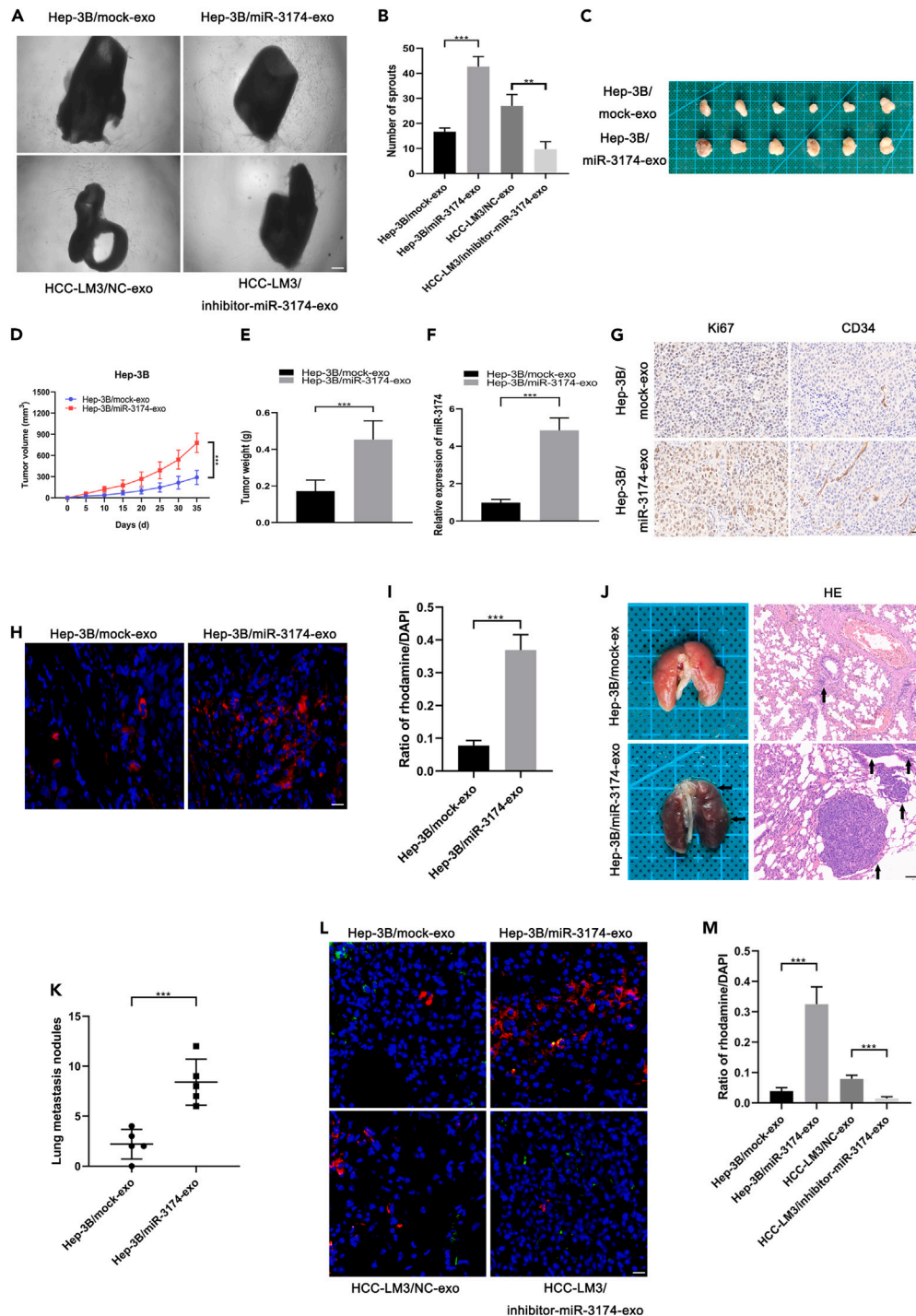


Figure 3. Exosomal miR-3174 promotes HCC progression and metastasis by inducing angiogenesis and enhancing vascular permeability in vivo

(A and B) Effect of exosomes derived from cells in four groups: Hep-3B/mock, Hep-3B/miR-3174, HCC-LM3/NC, and HCC-LM3/inhibitor-miR-3174 on vascular outgrowth of aortic rings. Vascular outgrowth was quantified by counting all sprouts from aortic rings. Error bars represent mean \pm SEM of three replicates (n = 3). Scale bar represents 100 μ m.

(C) Photographs of xenograft tumor obtained from the nude mice injected by exosomes derived from Hep-3B/mock and Hep-3B/miR-3174. (n = 6).

(D and E) Volumes and weights of the xenograft tumors in the groups of Hep-3B/mock-exo and Hep-3B/miR-3174-exo (n = 6).

(F) RT-qPCR analysis of miR-3174 expression levels in xenograft tumors in Hep-3B/mock-exo and Hep-3B/miR-3174-exo groups.

(G) Effect of exosomal miR-3174 on intratumoral microvessel density (CD34) and progression (Ki67) of xenograft tumors in the groups of Hep-3B/mock-exo and Hep-3B/miR-3174-exo: CD34 and Ki67 expression levels were measured by immunohistochemical staining. Scale bar represents 50 μ m.

Figure 3. Continued

(H and I) Effect of exosomal miR-3174 on vascular permeability in xenograft tumor tissues in the groups of Hep-3B/mock-exo and Hep-3B/miR-3174-exo. Intensities of rhodamine–dextran fluorescence in xenograft tumor tissues were quantified and normalized to the intensities of DAPI. Scale bar represents 50 μm . (J and K) Photographs and H&E staining images of lung metastasis tissues in Hep-3B/mock and Hep-3B/miR-3174 groups. The numbers of lung metastatic nodules (indicated by arrows) were counted under the microscope ($n = 5$). Scale bar represents 50 μm . (L and M) Effect of exosomal miR-3174 on vascular permeability in lung metastasis tissues of nude mice in the groups of Hep-3B/mock-exo, Hep-3B/miR-3174-exo, HCC-LM3/NC-exo, and HCC-LM3/inhibitor-miR-3174-exo. Intensities of rhodamine–dextran fluorescence in lung metastasis tissues were quantified and normalized to the levels of DAPI. Scale bar represents 50 μm . Error bars represent mean \pm SEM. (* $p < 0.05$, ** $p < 0.01$, *** $p < 0.001$).

(green) could bind to p53 (red) in the nuclei of HUVECs (DAPI) (Figure 4J). CO-IP assays further confirmed that HIPK3 is a binding partner of p53 in HUVECs transfected with HIPK3-flag plasmids (Figure 4K). Finally, western blot analysis and immunofluorescence staining also exhibited that the expression levels of HIPK3, p53, Fas, ZO-1, VE-cadherin (VE-cad), and cleaved Caspase-3 in HUVECs treated with Hep-3B/miR-3174-exo were decreased significantly but VEGFR-2 was upregulated. On the contrary, the opposite results appeared in HCC-LM3/inhibitor-miR-3174-exo group (Figures 4L and 4M). The above results revealed that exosomal miR-3174 can promote angiogenesis and enhance vascular permeability by inhibiting HIPK3/p53 and HIPK3/Fas signaling pathways.

The enhancement of exosomal miR-3174 on angiogenesis and vascular permeability can be reversed by HIPK3 or GW4869 *in vitro*

To investigate whether HIPK3 was essential in exosomal miR-3174-mediated angiogenesis and vascular permeability, we transfected HUVECs with HIPK3 overexpression plasmids (Hep-3B/miR-3174-exo+HIPK3) and treated Hep-3B cells with GW4869 to inhibit the secretion of exosomes (Hep-3B/miR-3174-exo+GW4869). Scratch healing assay and transwell migration assay showed that the migration of HUVECs could be inhibited by HIPK3 or GW4869 compared with that in Hep-3B/miR-3174-exo group (Figures 5A–5D). Angiogenesis of HUVECs was revealed to be weakened by HIPK3 or GW4869 in tube formation assay and 3D spheroid sprouting assay (Figures 5E–5H). In line with that, intervention of HIPK3 or GW4869 administration attenuated the enhancement of exosomal miR-3174 on vascular permeability (Figure 5I). Above all, HIPK3 was critical in exosomal miR-3174-induced angiogenesis and permeability of HUVECs.

The enhancement of exosomal miR-3174 on angiogenesis and metastasis can be reversed by HIPK3 or GW4869 *in vivo*

To further clarify the necessity of HIPK3 in miR-3174-induced alteration of vascular phenotypes, *in vivo* experiments were also performed. Aortic ring assay demonstrated that the ability of Hep-3B/miR-3174-exo to improve aortic ring budding was markedly inhibited by treatment with HIPK3 plasmids or GW4869 (Figures 6A and 6B). In xenograft tumor models, size and weight of the implanted tumors in Hep-3B/miR-3174-exo+HIPK3 group were lower than those in Hep-3B/miR-3174-exo group (Figures S2J–S2L). Immunohistochemical staining analysis showed that the expression levels of Ki67 and CD34 were decreased, whereas HIPK3 was upregulated in Hep-3B/miR-3174-exo+HIPK3 group (Figure S2L). Similarly, upregulation of HIPK3 also reduced the vascular permeability and fluorescence intensity of Rhodamine B in implanted tumors (Figures S2M and S2N). In the lung metastasis models, we also discovered that upregulation of HIPK3 or GW4869 treatment decreased the number of pulmonary metastatic nodules and the permeability of blood vessels (Figures 6C–6G). Immunofluorescence staining showed that in HIPK3 and GW4869 groups, CD34 was less evident, whereas HIPK3 was highly expressed in VECs of lung tissues compared with those in Hep-3B/miR-3174-exo group (Figure 6H). Western blot analysis and immunofluorescence staining of HUVECs revealed that in Hep-3B/miR-3174-exo+HIPK3 group and Hep-3B/miR-3174-exo+GW4869 group the expression levels of HIPK3, Fas, p53, VE-cad, ZO-1, and cleaved Caspase-3 were increased significantly, whereas VEGFR-2 was downregulated compared with those in Hep-3B/miR-3174-exo group (Figures 6I and 6J). Collectively, upregulation of HIPK3 or pretreatment with GW4869 could inhibit the enhancement of exosomal miR-3174 on angiogenesis and vascular permeability. The activation of HIPK3/p53 and HIPK3/Fas pathways further curbed the progression and metastasis of HCC.

Hypoxia induces HCC cells to secrete more exosomal miR-3174

Even that, we have demonstrated that exosomal miR-3174 can be secreted by HCC cells. The mechanisms of miR-3174 upregulation in HCC and how miR-3174 was packaged into exosomes remained indistinct. It is well known that hypoxia is a common factor to affect the expression levels and secretion of exosomal miRNAs in cancer cells.¹⁴ To confirm this inference, we discovered that exosomes secreted by Hep-3B cells in hypoxia (5% O_2) group were more than those in normoxia (20% O_2) group under the same visual field (Figure 7A). Western blot analysis exhibited that the exosomes isolated under normoxia or hypoxia were all positive for the markers of exosomes (ALIX, TSG101, CD63, and CD9) (Figure 7B). NTA analysis confirmed that the concentration of exosomes secreted by Hep-3B cells under hypoxia was higher than that under normoxia (Figure 7C). In addition, under hypoxia, more exosomes labeled with PKH67 were observed to be ingested by HUVECs (Figure 7D). Consistently, miR-3174 was found to be upregulated under hypoxia in Hep-3B and HCC-LM3 cells by RT-qPCR analysis (Figure 7E). As we all know, HIF-1 α and HIF-2 α are the most common transcriptional regulators to dominate the biological behavior of HCC under hypoxia. We supposed that HIF-1 α and HIF-2 α may be involved in controlling HCC exosome secretion. Under electron microscope, we observed that the exosomes derived from Hep-3B cells decreased obviously in HIF-1 α knocked down group (Si-HIF-1 α VS Si-NC-1) rather than that in HIF-2 α knocked down group (Si-HIF-2 α VS Si-NC-2) (Figure S3A), implying that HIF-1 α was mainly involved in regulation of HCC exosome secretion. To explore the mechanism of upregulation of miR-3174 in HCC cells caused by hypoxia, we queried the miRTrans database

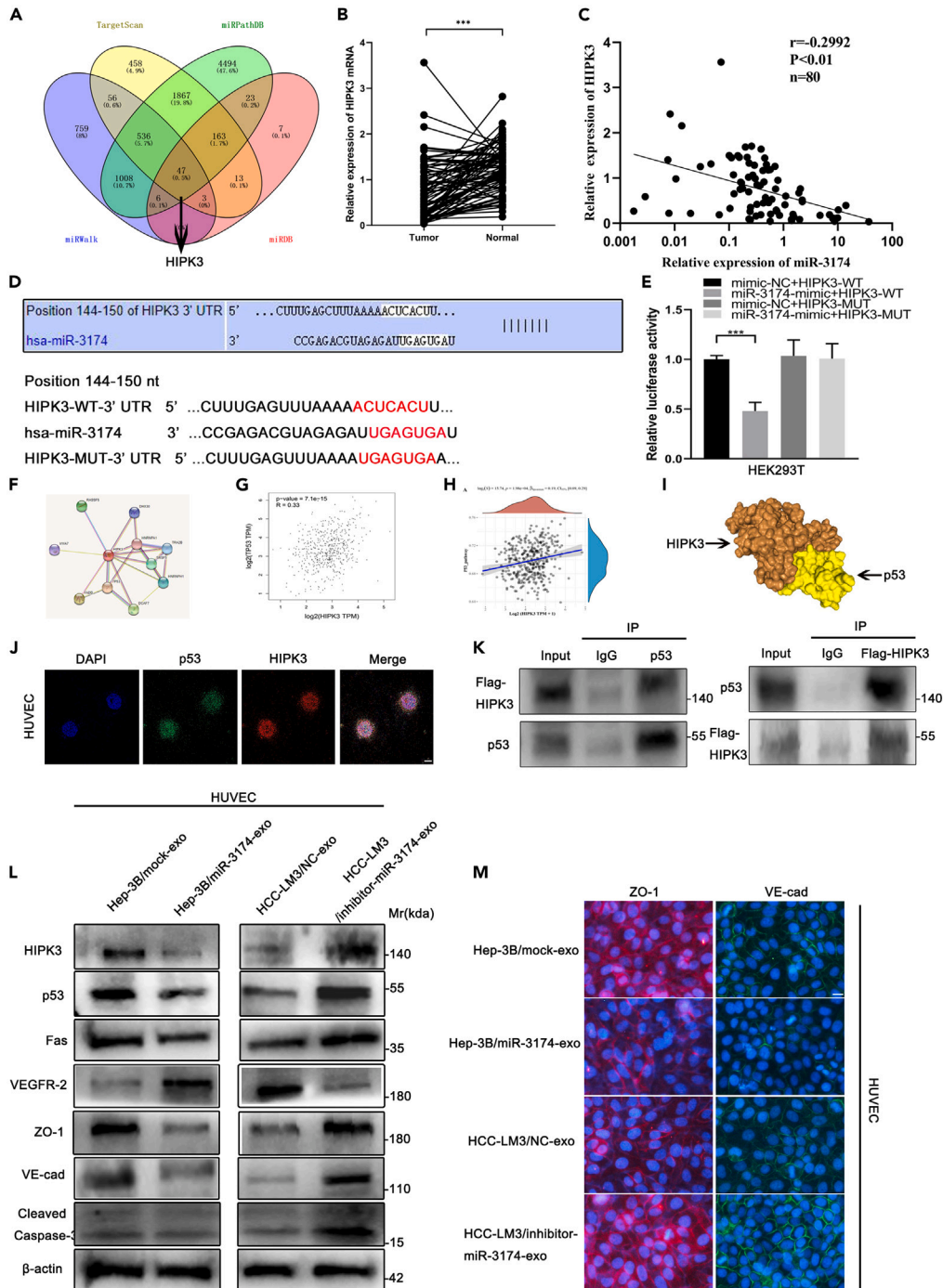


Figure 4. HCC-derived exosomal miR-3174 targetedly inhibits HIPK3/p53 signaling pathway in HUVECs

(A) Venn diagram displaying the potential target genes of miR-3174 predicted by four different prediction databases (TargetScan, miRWalk, miRDB, and miRPathDB).

(B) RT-qPCR analysis of HIPK3 expression levels in HCC tissues and adjacent normal liver tissues (n = 80).

(C) Pearson's correlation analysis of expression levels of miR-3174 and HIPK3 in HCC tissues (n = 80). Pearson's correlation coefficient (r) and p value are shown in the chart. p value is from Pearson's test.

(D) Original and mutated 3'UTR sites of HIPK3 potential to bind miR-3174 predicted by TargetScan database.

(E) Luciferase intensities of HEK293T cells co-transfected with WT HIPK3 3' -UTR or MUT HIPK3 3' -UTR and miR-3174 mimics or negative control oligoribonucleotides (mimic-NC) by dual luciferase report experiment.

(F) Predicted proteins' potential to interact with HIPK3 in STRING database.

Figure 4. Continued

(G) Pearson's correlation analysis of HIPK3 and TP53 expression levels in TCGA-LIHC database. Pearson's correlation coefficient (r) and p value are shown. p value is from Pearson's test.

(H) Spearman's correlation analysis of HIPK3 expression levels and p53 signaling pathway scores in TCGA-LIHC database. Spearman's correlation coefficient (r) and p value are shown. p value is from Spearman's test.

(I) The structural model of the binding of HIPK3 and p53 on HSYMDOCK Server.

(J) Colocalization analysis of HIPK3 (red) and p53 (green) in HUVECs (DAPI) by immunofluorescence staining. Scale bar represents 10 μ m.

(K) CO-IP assay performed to verify the binding of HIPK3 and p53 in HUVECs. (Left) Western blot analysis of HIPK3 (labeled with flag) and p53 expression levels in Input, anti-IgG, and anti-p53 (IP) groups. (Right) Western blot analysis of HIPK3 (labeled with flag) and p53 expression levels in Input, anti-IgG, and anti-HIPK3-Flag (IP) groups.

(L) Western blot analysis of expression levels of HIPK3, p53, Fas, VEGFR-2, ZO-1, VE-cad, and cleaved Caspase-3 in HUVECs incubated with exosomes derived from Hep-3B/mock, Hep-3B/miR-3174, HCC-LM3/NC, and HCC-LM3/inhibitor-miR-3174. β -actin was used as the loading control.

(M) The fluorescence intensities of ZO-1 (red) and VE-CAD (green) in HUVECs incubated with exosomes derived from Hep-3B/mock, Hep-3B/miR-3174, HCC-LM3/NC, and HCC-LM3/inhibitor-miR-3174 by immunofluorescence staining. Scale bar represents 25 μ m. Error bars represent Mean \pm SEM of three replicates (n = 3). (*p < 0.05, **p < 0.01, ***p < 0.001).

and found that HIF-1 α probably was the potential transcriptional regulator of miR-3174. Western blot analysis was performed to verify the upregulation of HIF-1 α in Hep-3B and HCC-LM3 cells under hypoxia (Figure 7F). The potential binding site of HIF-1 α and miR-3174 promoter region obtained from the JASPAR database was shown in the chart (Figure 7G). ChIP assay exhibited that HIF-1 α under hypoxia was enriched in the predicted binding sequence of miR-3174 promoter region as detected by agarose gel electrophoresis (Figure 7H). Further dual luciferase report experiment confirmed that the luciferase activity in HEK293T cells cotransfected with pcDNA-HIF-1A and miR-3174 pro-WT was abated significantly compared with other groups (Figure 7I). In summary, the abovementioned experimental results showed that HIF-1 α positively regulated the transcription of miR-3174 in HCC cells under hypoxia.

To clarify how miR-3174 was loaded into exosomes in HCC cells, we predicted the proteins potential to bind miR-3174 by the RBPDB database. The top three proteins potentially binding to miR-3174 were SFRS2, HNRNPA1, and ACO1 (Figure 7J). Then, we constructed siRNAs for these proteins respectively. The transfection efficiency was verified (Figures S3B–S3D). By analyzing the TCGA-LIHC database, we found that there was a significant positive correlation between HNRNPA1 and miR-3174 in HCC tissues (Figure S1E). Subsequent RT-qPCR analysis revealed that the expression level of miR-3174 in exosomes was downregulated dramatically in si-HNRNPA1 group, whereas the expression level of miR-3174 in Hep-3B cells changed inapparently (Figures S3E and S3F), suggesting that HNRNPA1 might be the critical regulator for the process of packaging miR-3174 into exosomes. Meanwhile, HNRNPA1 was found high-expressed in most cancer tissues including HCC in TCGA database (Figure S3G). The OS and disease-free survival (DFS) rates of HCC patients with high-expressed HNRNPA1 were lower than those in low-expressed group (Figures S3H and S3I). Interestingly, there was a strong positive correlation between HNRNPA1 and HIF1A in TCGA-LIHC database (Figure S1F), prompting us to speculate that HNRNPA1 might be modulated by hypoxia. As expected, both western blot analysis and immunofluorescence staining showed that the expression levels of HNRNPA1 were increased in Hep-3B and HCC-LM3 cells under hypoxia (Figures 7F and 7K). After silencing of HNRNPA1 in Hep-3B, exosomal miR-3174 labeled with Cy3 was decreased significantly in HUVECs (Figure 7L). RIP assay was applied to confirm that in anti-HNRNPA1 group, HNRNPA1 and miR-3174 were enriched significantly compared with immunoglobulin G (IgG) group (Figure 7M). Anyway, hypoxia-induced HIF-1 α and HNRNPA1 further promote the transcription and production of exosomal miR-3174 in HCC cells. A schema diagram was also drawn to illustrate the process of HCC-derived exosomal miR-3174 induced by hypoxia regulating angiogenesis and permeability of VECs (Figure 8).

The prognosis of HCC patients with high-expressed miR-3174 is poor

To further explore the correlation between miR-3174 and clinical features of HCC, we divided 80 HCC patients into two groups (n = 40) according to the median expression level of miR-3174. The detailed data are shown in Table 1. We found that high-expressed miR-3174 was positively associated with microvascular invasion (MVI) in HCC (Table 1). Then we discovered that the OS of HCC patients with high-expressed miR-3174 in TCGA-LIHC database was lower than that in the low-level group (Figure S1G). In addition, the area under curve (AUC) of miR-3174 reached 0.63 (Figure S1H). Kaplan-Meier (K-M) analysis revealed that OS of HCC patients with high-expressed miR-3174 was lower than that in the group with low-expressed miR-3174 (Figure S1I). To further verify our inference, these collected clinical data of HCC patients were all incorporated into the cox proportional hazards model. Univariate and multivariate analysis showed that miR-3174 and tumor size can be acted as independent predictors of OS of HCC patients (Table 2). Above all, miR-3174 might be a critical indicator for worse prognosis of HCC patients.

DISCUSSION

MiR-3174 has been a newly discovered miRNA involved in regulating the occurrence and progression of various malignant tumors in recent years. It has been reported that miR-3174 can drive the progression of cancers, including gastric cancer, HCC, and rectal cancer.^{12,15,16} For example, miR-3174 was reported to weaken apoptosis and autophagy of gastric cancer cells via inhibiting ARHGAP10/p53 signaling pathway.¹⁶ On the contrary, a few studies indicated that miR-3174 negatively regulated cancer progression.^{17,18} The research on bladder cancer exhibited that miR-3174 inhibited tumor proliferation by inhibiting ADAM15.¹⁸ However, previous studies mostly focused on the effects of miR-3174 on cancer cells, ignoring the possibility that miR-3174 can also regulate the crosstalk between cancer and other cells. Exosomes are

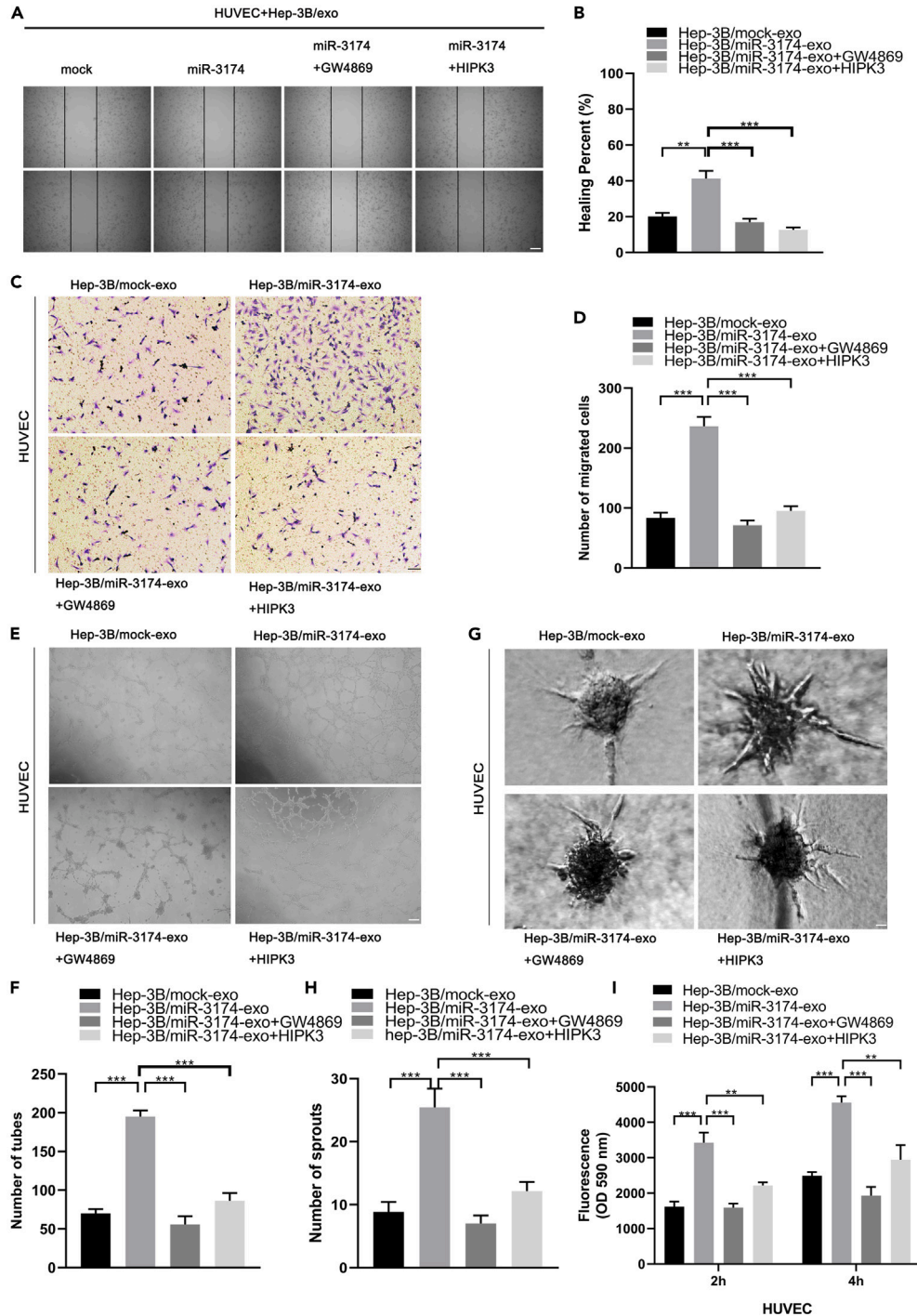


Figure 5. The enhancement of exosomal miR-3174 on angiogenesis and vascular permeability of HUVECs can be reversed by HIPK3 or GW4869 in vitro (A and B) The percent of healing area of HUVECs incubated with exosomes secreted by Hep-3B cells in four groups: mock, miR-3174, miR-3174+GW4869 and miR-3174+HIPK3 for 72h in scratch-healing assay. Scale bar represents 100 μ m. (C and D) Numbers of migrated HUVECs incubated with exosomes secreted by Hep-3B cells in abovementioned four groups in transwell migration assay. Scale bar represents 100 μ m. (E and F) Numbers of tubes formed by HUVECs incubated with exosomes secreted by Hep-3B cells in abovementioned four groups in tube formation assay. Scale bar represents 100 μ m.

Figure 5. Continued

(G and H) Numbers of sprouts formed by HUVEC spheroids cocultured with exosomes secreted by Hep-3B cells in abovementioned four groups for 48 h in 3D spheroid sprouting assay. Scale bar represents 50 μ m.

(I) Fluorescence intensities at OD 590 nm of HUVECs treated with rhodamine-dextran (70 kDa) detected at 2 h and 4 h after exposure to exosomes derived from Hep-3B cells in abovementioned four groups for 72 h. Error bars represent mean \pm SEM of three replicates (n = 3). (*p < 0.05, **p < 0.01, ***p < 0.001).

well-known important carriers that can transmit hereditary substances between cells in TME.¹⁹ In this study, we first revealed that exosomal miR-3174 delivered to VECs induces angiogenesis and impairs functional integrity of VECs, resulting in increased vascular permeability and metastasis. Exosomal miRNAs act as a bridge between HCC and VECs in TME. Except VECs, exosomal miRNAs secreted by cancer cells also affect multiple cells, including fibroblasts, macrophages, and neutrophils.^{20–22} For example, Yuan Ying et al.²⁰ found that exosomal miR-21-5p from colorectal cancer (CRC) induced macrophages to differentiate into tumor-associated M2 macrophages and upregulated PD-L1 to further assist the immune escape of CRC. Our study confirmed that ingesting HCC-derived exosomes, VECs can migrate and form new vascular cavities with destructed integrity. Neovascularization accelerates HCC progression and high leakiness of blood vessels is conducive to HCC metastasis.³ In short, our study explained that exosomal miR-3174 can be transmitted to VECs and participate in remodeling the surrounding neovascularizations to assist HCC progression and metastasis.

By bioinformatic analysis, we predicted that the target gene of miR-3174 was HIPK3, and it has been proven by dual luciferase reporter assay. HIPK3 is subordinate to the family of homologous domain interacting protein kinases (HIPKs) in the GMSC kinase group. HIPKs are composed of HIPK1–4.²³ The relationship among HIPK1–3 is the most intimate, of which approximately 87% sequences in their kinase domains are consistent.²³ HIPK1–3 interacts with other proteins sharing a complex domain system, especially the C-terminal of a region rich in serine, glutamate, and alanine (SQA) residues.²⁴ Recent studies have confirmed that HIPK3 is involved in mediating proliferation, angiogenesis, apoptosis, and signal transduction of cancer cells.¹³ Previous studies have proven that HIPK2 in HIPKs family can activate p53 signaling pathway to inhibit the progression and angiogenesis of cancers.²⁵ P53 signaling pathway plays an important role in regulating migration, permeability, and angiogenesis of VECs. P53 in VECs inhibits the abnormal formation of blood vessels and the increases of leakage effectively.²⁶ Given that, we speculated that HIPK3, highly homologous to HIPK2, might activate p53 pathway. Combined with bioinformatic analysis and experimental results, we verified for the first time that HIPK3 regulates angiogenesis and permeability via p53 pathway in VECs. Moreover, HIPK3 was also known to mediate cell proliferation and apoptosis through Fas signaling pathway.²⁷ In our study, we also found that miR-3174 inhibited the HIPK3/Fas signaling pathway, thus promoting the angiogenesis and proliferation of HUVECs. Above all, HIPK3 plays an important role in inhibiting angiogenesis and permeability of VECs.

Interestingly, miRNAs in exosomes are not randomly selected by HCC cells. The process of transcription and packaging of miRNA into exosomes is monitored by complex regulatory mechanisms.²⁶ Exosomal miRNAs are important components of TME and easily affected by environmental changes in TME. For example, hypoxia stimulates the production of exosomes and induces HIF-1 α to promote the transcription of miRNAs packaged into exosomes.^{19,28} In our study, we confirmed that hypoxia induces the upregulation of HIF-1 α in HCC cells, which then accelerates the releases of exosomes and enhances the transcription of miR-3174. Similarly, the process of miR-3174 transported into exosomes is also regulated by RNA-binding proteins (RBP) named HNRNPA1. Heterogeneous nuclear ribonucleoproteins (HNRNPs) are important proteins that control the packaging of cargoes into exosomes.²⁹ It has been proven that HNRNPA1 is involved in the sorting of miRNAs into exosomes.³⁰ In this study, we proved that HNRNPA1 can be upregulated by hypoxia and promotes miR-3174 loaded into exosomes. Anyway, our study revealed that hypoxia can induce HCC cells to secrete more exosomal miR-3174 by upregulating HIF-1 α and HNRNPA1.

In summary, our study has further confirmed that exosomal miR-3174 can promote angiogenesis and metastasis of HCC by inhibiting HIPK3 in VECs. Under hypoxia, HIF-1 α and HNRNPA1 can promote the secretion of exosomal miR-3174 in HCC cells. However, there are still some deficiencies in this study. First, we failed to collect enough peripheral blood samples from HCC patients to further analyze the expression levels of exosomal miR-3174 in the blood of HCC patients. In addition, we have not synthesized a blocking drug of exosomal miR-3174 to prevent its transmission to vascular endothelial cells. Our study revealed a new mechanism by which HCC-derived exosomes regulate angiogenesis and permeability of blood vessels. Exosomal miR-3174 may become a new monitoring indicator or therapeutic target for HCC.

STAR★METHODS

Detailed methods are provided in the online version of this paper and include the following:

- KEY RESOURCES TABLE
- RESOURCE AVAILABILITY
 - Lead contact
 - Materials availability
 - Data and code availability
- EXPERIMENTAL MODEL AND STUDY PARTICIPANT DETAILS
 - Animal care ethics statement
- METHOD DETAILS
 - Patients, tissues and follow-up
 - Cell lines and culture
 - Isolation and identification of exosomes from HCC cells

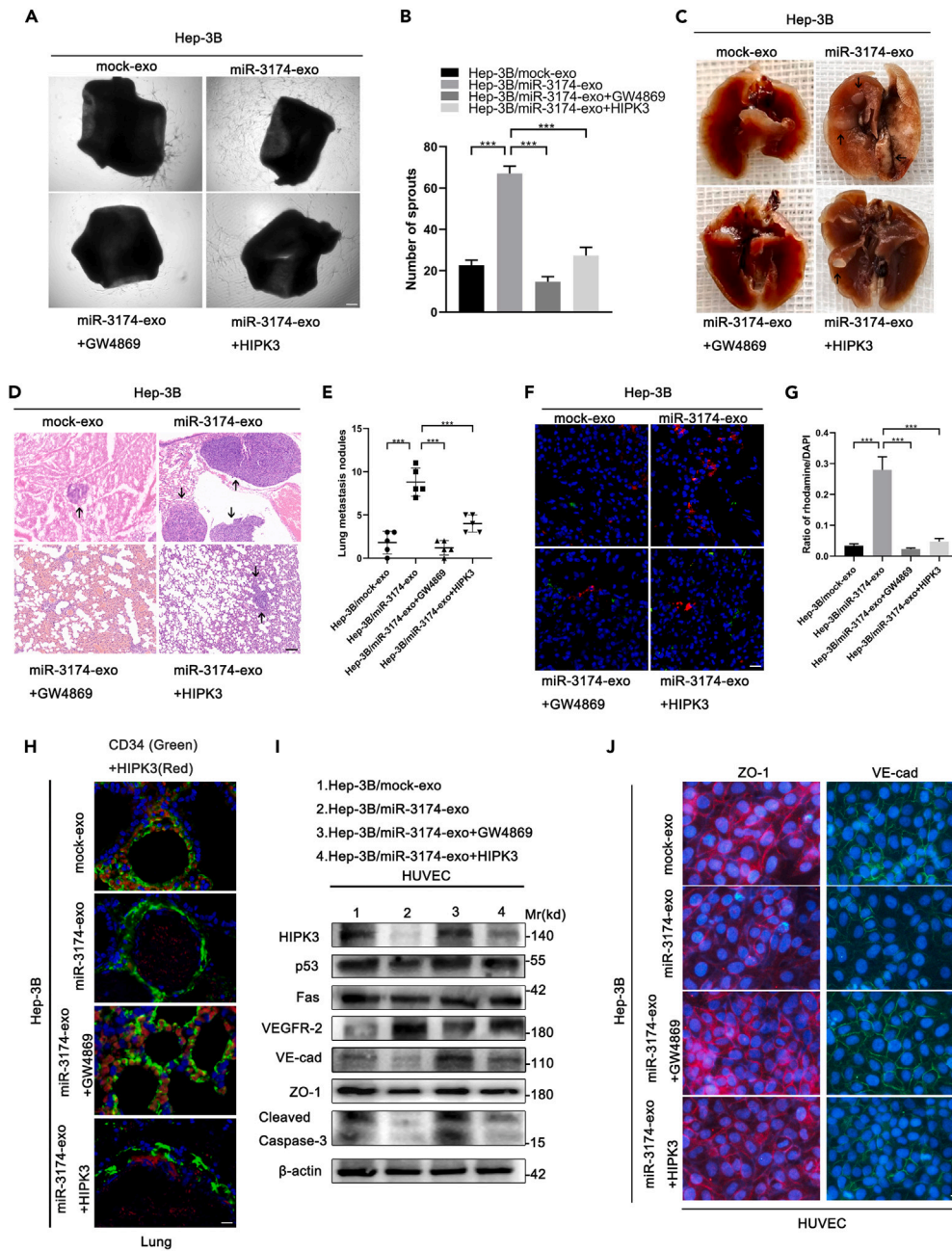


Figure 6. The enhancement of exosomal miR-3174 on angiogenesis and metastasis of HCC can be reversed by HIPK3 *in vivo*

(A and B) Effect of exosomes derived from Hep-3B cells in four groups: mock, miR-3174, miR-3174+GW4869, and miR-3174+HIPK3 on vascular outgrowth of aortic rings. Vascular outgrowth was quantified by counting the sprouts formed by aortic rings. Error bars represent mean \pm SEM of three replicates (n = 3). Scale bar represents 100 μ m.

(C–E) Photographs and H&E staining images of lung metastasis obtained from the nude mice injected by Hep-3B-cell-derived exosomes in abovementioned four groups. The numbers of lung metastatic nodules (indicated by arrows) were also shown in the chart (n = 5). Scale bar represents 50 μ m.

(F and G) Effect of exosomal miR-3174 on vascular permeability in lung metastasis tissues of nude mice in abovementioned four groups. Intensities of rhodamine-dextran fluorescence in lung metastasis tissues were quantified and normalized to the intensities of DAPI (n = 5). Scale bar represents 50 μ m.

(H) The fluorescence staining analysis of CD34 (green) and HIPK3 (red) in lung tissues (DAPI) in abovementioned four groups. Scale bar represents 50 μ m.

(I) Western blot analysis of expression levels of HIPK3, p53, Fas, VEGFR-2, ZO-1, VE-cad, and cleaved Caspase-3 in HUVECs in abovementioned four groups for 48 h. β -actin was used as the loading control.

(J) The fluorescence staining analysis of ZO-1 (red) and VE-CAD (green) in HUVECs in abovementioned four groups. Scale bar represents 25 μ m. Error bars represent mean \pm SEM. (*p < 0.05, **p < 0.01, ***p < 0.001).

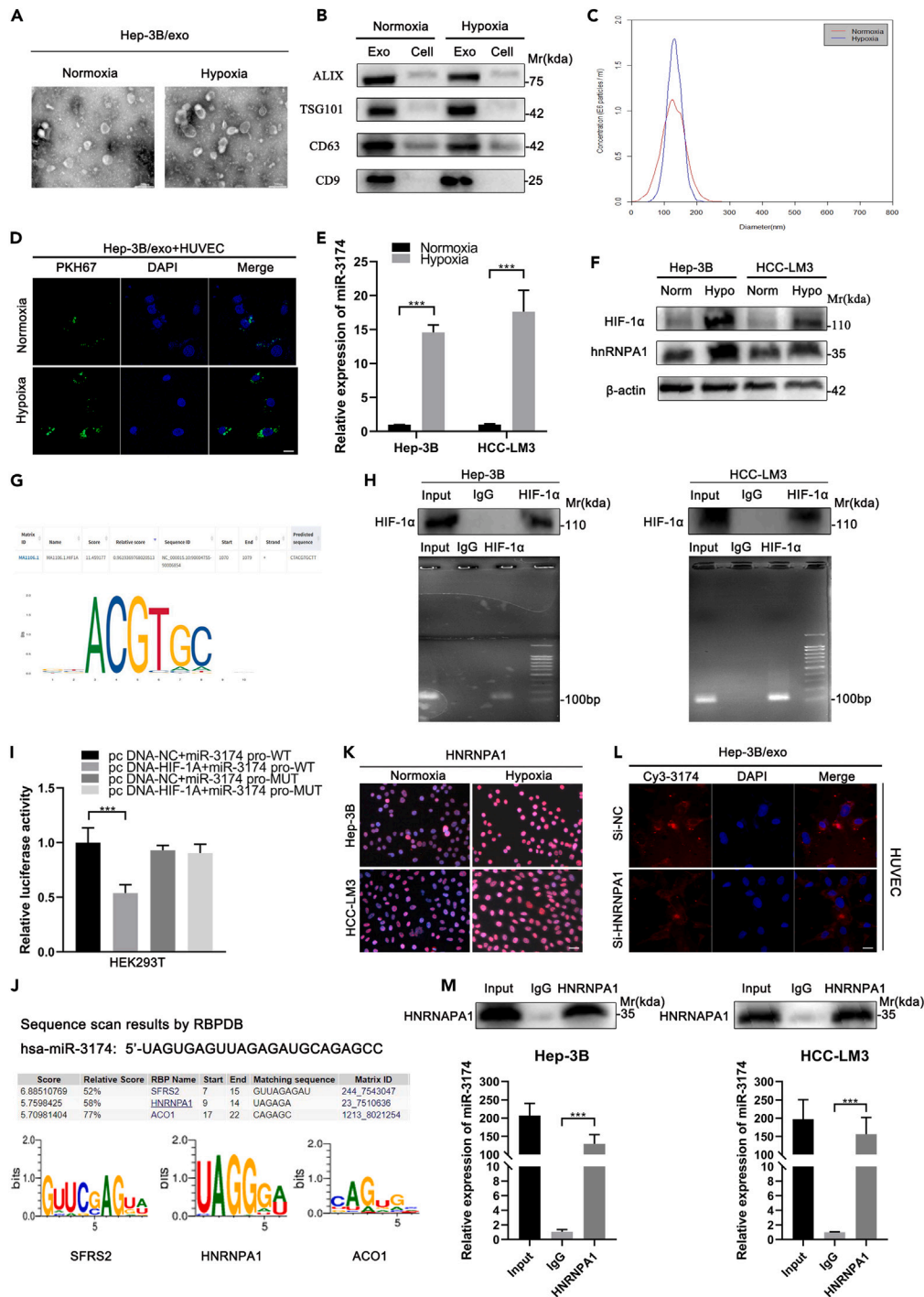


Figure 7. Hypoxia induces HCC to secrete more exosomal miR-3174

(A) Electron micrographs of exosomes derived from Hep-3B cells cultured under normoxia and hypoxia for 48 h. Scale bar represents 200 nm.
 (B) Western blot analysis of expression levels of exosome markers (ALIX, TSG101, CD63, CD9) in Hep-3B cells and cell-derived exosomes cultured under normoxia and hypoxia for 48 h.
 (C) NTA analysis of the abundance of exosomes derived from Hep-3B cells cultured under normoxia and hypoxia for 48 h.
 (D) Exosomes labeled with PKH67 (green) derived from Hep-3B cells cultured under normoxia and hypoxia for 48 h ingested by HUVECs (DAPI). Scale bar represents 25 μ m.
 (E) RT-qPCR analysis of miR-3174 expression levels in Hep-3B cells and HCC-LM3 cells cultured under normoxia and hypoxia for 48 h.

Figure 7. Continued

(F) Western blot analysis of expression levels of HIF-1 α and HNRNPA1 in Hep-3B and HCC-LM3 cells cultured under normoxia and hypoxia for 48 h. β -actin was used as the loading control.

(G) The sites of HIF-1 α potential to bind to the promoter region of miR-3174 predicted by the JASPAR database.

(H) The ChIP assay was performed using primers specific for the predicted binding site of HIF-1 α and promoter region of miR-3174 in Hep-3B and HCC-LM3 cells cultured under hypoxia for 48 h. The expression levels of IP products in Input, IgG, and anti-HIF-1 α groups were detected by western blot analysis (top). The expression levels of PCR products were analyzed by agarose gel electrophoresis (bottom).

(I) Luciferase activities of HEK293T cells cotransfected with pcDNA-NC or pcDNA-HIF-1A together with miR-3174 pro-WT or miR-3174 pro-MUT in dual luciferase report assay.

(J) (Top) The top 3 RNA-binding proteins' potential to interact with miR-3174 predicted by RBPDB database (threshold = 0.5). (Bottom) The specific binding sites of RNA-binding proteins: SFRS2, HNRNPA1, and ACO1.

(K) The fluorescence intensities of HNRNPA1 (red) in Hep-3B and HCC-LM3 cells (DAPI) cultured under normoxia and hypoxia for 48 h were analyzed by immunofluorescence staining. Scale bar represents 25 μ m.

(L) Exosomal miR-3174 labeled with Cy3 (red) ingested by HUVECs (DAPI) in Si-NC and Si-HNRNPA1 groups. The exosomes were isolated from Hep-3B cells cotransfected with miR-3174 mimics-Cy3 and Si-NC or Si-HNRNPA1 for 48 h. Scale bar represents 25 μ m.

(M) The RIP assay was performed to verify the predicted binding of HNRNPA1 and miR-3174 in Hep-3B and HCC-LM3 cells cultured under hypoxia for 48 h. (Top) The expression levels of IP products in Input, IgG, and anti-HNRNPA1 groups were detected by western blot analysis. (Bottom) The expression levels of miR-3174 in Input, IgG, and anti-HNRNPA1 groups were measured by qRT-PCR. Error bars represent mean \pm SEM of three replicates. (*p < 0.05, **p < 0.01, ***p < 0.001).

- Transfection and treatment of HCC-derived exosomes
- Scratch-healing assay
- Transwell migration assay
- Tube formation assay
- 3D spheroid sprouting assay
- *In vitro* HUVECs permeability assay
- Aortic ring assay
- Animal disease models and *in vivo* vascular permeability assay
- Dual luciferase reporter assay
- Immunohistochemical and immunofluorescent staining
- Co-Immunoprecipitation (CO-IP) assay
- Chromatin immunoprecipitation (ChIP) assay
- RNA immunoprecipitation (RIP) assay
- Quantitative real-time polymerase chain reaction (qRT-PCR)
- Western blot (WB) analysis
- Bioinformatics analysis and online public databases
- **QUANTIFICATION AND STATISTICAL ANALYSIS**

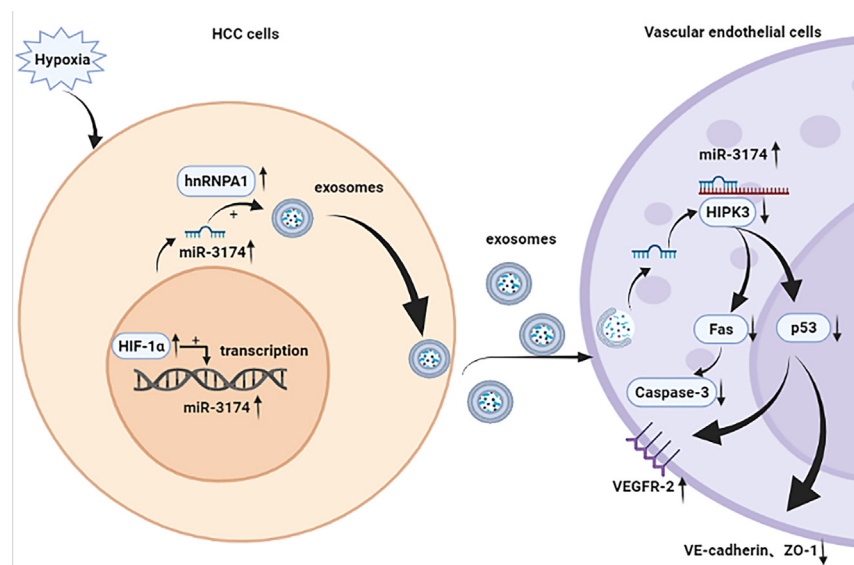


Figure 8. A schema diagram illustrating the role of HCC-derived exosomal miR-3174 induced by hypoxia in regulating angiogenesis and permeability of VECs

Table 1. Correlation between expression levels of miR-3174 and clinicopathological features of HCC patients

Clinicopathological parameters	Number	Low (n = 40)	High (n = 40)	p value
		miR-3174	miR-3174	
Age(years)	80			0.284
≤60	18	7	11	
>60	62	33	29	
Gender	80			0.210
Female	12	8	4	
male	68	32	36	
Liver cirrhosis	80			0.446
Yes	59	28	31	
No	21	12	9	
HBsAg	80			0.446
Positive	59	28	31	
Negative	21	12	9	
Virus titer (copies/mL)	80			0.805
≤100	57	28	29	
>100	23	12	11	
AFP (ng/mL)	80			0.496
≤20	33	18	15	
>20	47	22	25	
DCP (ng/mL)	80			0.340
≤40	54	25	29	
>40	26	15	11	
Tumor size (cm)	80			0.369
≤5	44	24	20	
>5	36	16	20	
Tumor multiplicity	80			0.499
Single	70	34	36	
Multiple	10	6	4	
Microvascular invasion	80			0.022 ^a
Yes	21	6	15	
No	59	34	25	
Edmondson grade	80			0.302
I-II	60	32	28	
III-IV	20	8	12	
TNM stage	80			0.633
I-II	54	28	26	
III-IV	26	12	14	

^aIndicates p < 0.05; AFP, a-fetoprotein; DCP, des-γ-carboxy prothrombin.

SUPPLEMENTAL INFORMATION

Supplemental information can be found online at <https://doi.org/10.1016/j.isci.2024.108955>.

ACKNOWLEDGMENTS

This study was supported by the National Natural Science Foundation of China Project (81871260) and Science and Technology Development Fund of Xuzhou Medical University (XYFY2020045).

Table 2. Univariate and multivariate analyses of factors associated with overall survival of HCC patients in Cox proportional-hazards model

Clinical variables	Case number	HR (95% CI) ^a	p value ^a
Univariate analysis			
MiR-3174 (low versus high)	40/40	2.4 (1.1–8.2)	0.025 ^b
Age (years) (≤60 versus >60)	62/18	1.2 (0.5–2.9)	0.737
Gender (F versus M)	12/68	1.4 (0.4–4.5)	0.613
Liver cirrhosis (Yes versus No)	59/21	1.1 (0.5–2.6)	0.773
HBsAg (positive versus negative)	59/21	2.3 (0.9–6.1)	0.092
Virus titer (copies/mL) (≤100 versus >100)	57/23	1.9 (0.9–4.0)	0.084
AFP (ng/mL) (≤20 versus >20)	33/47	2.8 (1.2–6.6)	0.018 ^b
DCP (ng/mL) (≤40 versus >40)	54/26	1.0 (0.4–2.2)	0.971
Tumor size (cm) (≤5 versus >5)	44/36	4.3 (1.7–10.7)	0.002 ^b
Tumor multiplicity (single versus multiple)	70/10	1.2 (0.5–3.0)	0.702
Microvascular invasion (Yes versus No)	21/59	3.1 (1.4–6.6)	0.004 ^b
Edmondson grade (I–II versus III–IV)	60/20	2.0 (1.0–4.3)	0.063
TNM stage (I–II versus III–IV)	54/26	2.4 (1.1–4.9)	0.022 ^b
Multivariate analysis			
MiR-3174 (low versus high)	40/40	2.3 (1.0–4.9)	0.038 ^b
Tumor size (cm) (≤5 versus >5)	44/36	3.5 (1.4–8.8)	0.009 ^b

^aHR, hazard ratio; 95% CI, 95% confidence interval.

AUTHOR CONTRIBUTIONS

X.Y., L.K., and W.J. designed this study. X.Y. and X.K. performed the experiments and bioinformatics analysis. Y.W., C.H., and D.Z. collected and analyzed the experimental and clinical data. X.Y. wrote the paper. F.Q., M.W., and L.K. revised the article and performed supplementary experiments.

DECLARATION OF INTERESTS

All the authors declare that they have no competing interests.

Received: March 5, 2023

Revised: November 11, 2023

Accepted: January 15, 2024

Published: January 19, 2024

REFERENCES

- Fang, J.H., Zhang, Z.J., Shang, L.R., Luo, Y.W., Lin, Y.F., Yuan, Y., and Zhuang, S.M. (2018). Hepatoma cell-secreted exosomal microRNA-103 increases vascular permeability and promotes metastasis by targeting junction proteins. *Hepatology* 68, 1459–1475. <https://doi.org/10.1002/hep.29920>.
- De Toro, J., Herschlik, L., Waldner, C., and Mongini, C. (2015). Emerging roles of exosomes in normal and pathological conditions: new insights for diagnosis and therapeutic applications. *Front. Immunol.* 6, 203. <https://doi.org/10.3389/fimmu.2015.00203>.
- Zeng, Z., Li, Y., Pan, Y., Lan, X., Song, F., Sun, J., Zhou, K., Liu, X., Ren, X., Wang, F., et al. (2018). Cancer-derived exosomal miR-25-3p promotes pre-metastatic niche formation by inducing vascular permeability and angiogenesis. *Nat. Commun.* 9, 5395. <https://doi.org/10.1038/s41467-018-07810-w>.
- Boyiadzis, M., and Whiteside, T.L. (2015). Information transfer by exosomes: A new frontier in hematologic malignancies. *Blood Rev.* 29, 281–290. <https://doi.org/10.1016/j.blre.2015.01.004>.
- Shephard, A.P., Giles, P., Mbengue, M., Alraies, A., Spary, L.K., Kynaston, H., Gurney, M.J., Falcón-Pérez, J.M., Royo, F., Tabi, Z., et al. (2021). Stroma-derived extracellular vesicle mRNA signatures inform histological nature of prostate cancer. *J. Extracell. Vesicles* 10, e12150. <https://doi.org/10.1002/jev2.12150>.
- You, Y., Tian, Z., Du, Z., Wu, K., Xu, G., Dai, M., Wang, Y., and Xiao, M. (2022). M1-like tumor-associated macrophages cascade a mesenchymal/stem-like phenotype of oral squamous cell carcinoma via the IL6/Stat3/THBS1 feedback loop. *J. Exp. Clin. Cancer Res.* 41, 10. <https://doi.org/10.1186/s13046-021-02222-z>.
- Wang, H., Wei, H., Wang, J., Li, L., Chen, A., and Li, Z. (2020). MicroRNA-181d-5p-Containing Exosomes Derived from CAFs Promote EMT by Regulating CDX2/HOXA5 in Breast Cancer. *Mol. Ther. Nucleic Acids* 19, 654–667. <https://doi.org/10.1016/j.omtn.2019.11.024>.
- Wei, K., Ma, Z., Yang, F., Zhao, X., Jiang, W., Pan, C., Li, Z., Pan, X., He, Z., Xu, J., et al. (2022). M2 macrophage-derived exosomes promote lung adenocarcinoma progression by delivering miR-942. *Cancer Lett.* 526, 205–216. <https://doi.org/10.1016/j.canlet.2021.10.045>.
- Fang, T., Lv, H., Lv, G., Li, T., Wang, C., Han, Q., Yu, L., Su, B., Guo, L., Huang, S., et al. (2018). Tumor-derived exosomal miR-1247-3p induces cancer-associated fibroblast activation to foster lung metastasis of liver

- cancer. *Nat. Commun.* 9, 191. <https://doi.org/10.1038/s41467-017-02583-0>.
10. Lu, Y., Han, G., Zhang, Y., Zhang, L., Li, Z., Wang, Q., Chen, Z., Wang, X., and Wu, J. (2023). M2 macrophage-secreted exosomes promote metastasis and increase vascular permeability in hepatocellular carcinoma. *Cell Commun. Signal.* 21, 299. <https://doi.org/10.1186/s12964-022-00872-w>.
 11. Zhang, B., Sun, C., Liu, Y., Bai, F., Tu, T., and Liu, Q. (2022). Exosomal miR-27b-3p Derived from Hypoxic Cardiac Microvascular Endothelial Cells Alleviates Rat Myocardial Ischemia/Reperfusion Injury through Inhibiting Oxidative Stress-Induced Pyroptosis via Foxo1/GSDMD Signaling. *Oxid. Med. Cell. Longev.* 2022, 8215842. <https://doi.org/10.1155/2022/8215842>.
 12. Wang, Q., Yang, X., Zhou, X., Wu, B., Zhu, D., Jia, W., Chu, J., Wang, J., Wu, J., and Kong, L. (2020). MiR-3174 promotes proliferation and inhibits apoptosis by targeting FOXO1 in hepatocellular carcinoma. *Biochem. Biophys. Res. Commun.* 526, 889–897. <https://doi.org/10.1016/j.bbrc.2020.03.152>.
 13. Conte, A., and Pierantoni, G.M. (2018). Update on the Regulation of HIPK1, HIPK2 and HIPK3 Protein Kinases by microRNAs. *MicroRNA* 7, 178–186. <https://doi.org/10.2174/2211536607666180525102330>.
 14. Chen, K., Wang, Q., Liu, X., Wang, F., Yang, Y., and Tian, X. (2022). Hypoxic pancreatic cancer derived exosomal miR-30b-5p promotes tumor angiogenesis by inhibiting GJA1 expression. *Int. J. Biol. Sci.* 18, 1220–1237. <https://doi.org/10.7150/ijbs.67675>.
 15. Zhang, D.L., and Yang, N. (2019). MiR-3174 functions as an oncogene in rectal cancer by targeting PCBD2. *Eur. Rev. Med. Pharmacol. Sci.* 23, 2417–2426.
 16. Li, B., Wang, L., Li, Z., Wang, W., Zhi, X., Huang, X., Zhang, Q., Chen, Z., Zhang, X., He, Z., et al. (2017). miR-3174 Contributes to Apoptosis and Autophagic Cell Death Defects in Gastric Cancer Cells by Targeting ARHGAP10. *Mol. Ther. Nucleic Acids* 9, 294–311. <https://doi.org/10.1016/j.omtn.2017.10.008>.
 17. Li, Q.Y., Shen, J.Q., Li, J.H., Dai, D.F., Saeed, M., and Li, C.X. (2021). LINC00958/miR-3174/PHF6 axis is responsible for triggering proliferation, migration and invasion of endometrial cancer. *Eur. Rev. Med. Pharmacol. Sci.* 25, 6853–6861.
 18. Yu, C., Wang, Y., Liu, T., Sha, K., Song, Z., Zhao, M., and Wang, X. (2020). The microRNA miR-3174 Suppresses the Expression of ADAM15 and Inhibits the Proliferation of Patient-Derived Bladder Cancer Cells. *Oncotargets Ther.* 13, 4157–4168. <https://doi.org/10.2147/OTT.S246710>.
 19. Ge, L., Xun, C., Li, W., Jin, S., Liu, Z., Zhuo, Y., Duan, D., Hu, Z., Chen, P., and Lu, M. (2021). Extracellular vesicles derived from hypoxia-preconditioned olfactory mucosa mesenchymal stem cells enhance angiogenesis via miR-612. *J. Nanobiotechnol.* 19, 380. <https://doi.org/10.1186/s12951-021-01126-6>.
 20. Yin, Y., Liu, B., Cao, Y., Yao, S., Liu, Y., Jin, G., Qin, Y., Chen, Y., Cui, K., Zhou, L., et al. (2022). Colorectal Cancer-Derived Small Extracellular Vesicles Promote Tumor Immune Evasion by Upregulating PD-L1 Expression in Tumor-Associated Macrophages. *Adv. Sci.* 9, 2102620. <https://doi.org/10.1002/adv.202102620>.
 21. Qi, M., Xia, Y., Wu, Y., Zhang, Z., Wang, X., Lu, L., Dai, C., Song, Y., Xu, K., Ji, W., and Zhan, L. (2022). Lin28B-high breast cancer cells promote immune suppression in the lung pre-metastatic niche via exosomes and support cancer progression. *Nat. Commun.* 13, 897. <https://doi.org/10.1038/s41467-022-28438-x>.
 22. Scognamiglio, I., Cocca, L., Puoti, I., Palma, F., Ingenito, F., Quintavalle, C., Affinito, A., Roscigno, G., Nuzzo, S., Chianese, R.V., et al. (2022). Exosomal microRNAs synergistically trigger stromal fibroblasts in breast cancer. *Mol. Ther. Nucleic Acids* 28, 17–31. <https://doi.org/10.1016/j.omtn.2022.02.013>.
 23. Kaltheuner, I.H., Anand, K., Moecking, J., Düster, R., Wang, J., Gray, N.S., and Geyer, M. (2021). Abemaciclib is a potent inhibitor of DYRK1A and HIP kinases involved in transcriptional regulation. *Nat. Commun.* 12, 6607. <https://doi.org/10.1038/s41467-021-26935-z>.
 24. Kim, Y.H., Choi, C.Y., Lee, S.J., Conti, M.A., and Kim, Y. (1998). Homeodomain-interacting protein kinases, a novel family of co-repressors for homeodomain transcription factors. *J. Biol. Chem.* 273, 25875–25879. <https://doi.org/10.1074/jbc.273.40.25875>.
 25. D’Orazi, G., Rinaldo, C., and Soddu, S. (2012). Updates on HIPK2: a resourceful oncosuppressor for clearing cancer. *J. Exp. Clin. Cancer Res.* 31, 63.
 26. Chen, Y., Dang, J., Lin, X., Wang, M., Liu, Y., Chen, J., Chen, Y., Luo, X., Hu, Z., Weng, W., et al. (2022). RA Fibroblast-Like Synoviocytes Derived Extracellular Vesicles Promote Angiogenesis by miRNA-1972 Targeting p53/mTOR Signaling in Vascular Endothelium. *Front. Immunol.* 13, 793855. <https://doi.org/10.3389/fimmu.2022.793855>.
 27. Rochat-Steiner, V., Becker, K., Micheau, O., Schneider, P., Burns, K., and Tschopp, J. (2000). FIST/HIPK3: a Fas/FADD-interacting serine/threonine kinase that induces FADD phosphorylation and inhibits fas-mediated Jun NH(2)-terminal kinase activation. *J. Exp. Med.* 192, 1165–1174. <https://doi.org/10.1084/jem.192.8.1165>.
 28. Prieto-Vila, M., Yoshioka, Y., and Ochiya, T. (2021). Biological Functions Driven by mRNAs Carried by Extracellular Vesicles in Cancer. *Front. Cell Dev. Biol.* 9, 620498. <https://doi.org/10.3389/fcell.2021.620498>.
 29. Pan, Z., Zhao, R., Li, B., Qi, Y., Qiu, W., Guo, Q., Zhang, S., Zhao, S., Xu, H., Li, M., et al. (2022). EWSR1-induced circNEIL3 promotes glioma progression and exosome-mediated macrophage immunosuppressive polarization via stabilizing IGF2BP3. *Mol. Cancer* 21, 16. <https://doi.org/10.1186/s12943-021-01485-6>.
 30. Zhang, H., Deng, T., Liu, R., Ning, T., Yang, H., Liu, D., Zhang, Q., Lin, D., Ge, S., Bai, M., et al. (2020). CAF secreted miR-522 suppresses ferroptosis and promotes acquired chemoresistance in gastric cancer. *Mol. Cancer* 19, 43. <https://doi.org/10.1186/s12943-020-01168-8>.
 31. Théry, C., Witwer, K.W., Aikawa, E., Alcaraz, M.J., Anderson, J.D., Andriantsitohaina, R., Antoniou, A., Arab, T., Archer, F., Atkin-Smith, G.K., et al. (2018). Minimal information for studies of extracellular vesicles 2018 (MISEV2018): a position statement of the International Society for Extracellular Vesicles and update of the MISEV2014 guidelines. *J. Extracell. Vesicles* 7, 1535750. <https://doi.org/10.1080/20013078.2018.1535750>.
 32. Zhang, D., Lee, H., Zhu, Z., Minhas, J.K., and Jin, Y. (2017). Enrichment of selective miRNAs in exosomes and delivery of exosomal miRNAs in vitro and in vivo. *Am. J. Physiol. Lung Cell Mol. Physiol.* 312, L110–L121. <https://doi.org/10.1152/ajplung.00423.2016>.
 33. Zhang, Y., Liu, J., Zou, T., Qi, Y., Yi, B., Dissanayaka, W.L., and Zhang, C. (2021). DPSCs treated by TGF-beta1 regulate angiogenic sprouting of three-dimensionally co-cultured HUVECs and DPSCs through VEGF-Ang-Tie2 signaling. *Stem Cell Res. Ther.* 12, 281. <https://doi.org/10.1186/s13287-021-02349-y>.

STAR★METHODS

KEY RESOURCES TABLE

REAGENT or RESOURCE	SOURCE	IDENTIFIER
Antibodies		
VE-cadherin	Abcam	Cat# ab313632; RRID: AB_313632
ZO-1	Abcam	Cat# ab307799; RRID: N/A
TSG101	Abcam	Cat# ab125011; RRID: AB_10974262
VEGFR-2	Abcam	Cat# ab315238; RRID: N/A
Fas	Abcam	Cat# ab133619; RRID: AB_2940837
p53	Abcam	Cat# ab26; RRID: AB_303198
HIPK3	Abcam	Cat# ab72538; RRID: AB_1269085
Caspase-3	Abcam	Cat# ab32351; RRID: AB_725946
HIF-1 α	Abcam	Cat# ab179483; RRID: AB_2732807
DDDDK tag	Abcam	Cat# ab205606; RRID: AB_2916341
CD9	Abcam	Cat# ab236630; RRID: AB_2922400
CD63	Abcam	Cat# ab134045; RRID: AB_2800495
ALIX	Abcam	Cat# ab275377; RRID: N/A
SFRS2	Abcam	Cat# ab204916; RRID: AB_2909393
ACO-1	Abcam	Cat# ab183721; RRID: N/A
Ki-67	Abcam	Cat# ab15580; RRID: AB_443209
IgG	Abcam	Cat# ab172730; RRID: AB_2687931
β -actin	Proteintech	Cat# 81115-1-RR; RRID: AB_2923704
HRP-IgG	Proteintech	Cat# SA00001-2; RRID: AB_2722564
CD-34	Servicebio	Cat# GB111693-100; RRID: N/A
HNRNPA1	ABclonal	Cat# A11564; RRID: AB_2861599
Experimental models: Cell lines		
Hep-3B	Pricella	Cat# CL-0102; RRID: N/A
HCC-LM3	Pricella	Cat# CL-0278; RRID: N/A
HEK293T	Pricella	Cat# CL-0005; RRID: N/A
PUMC-HUVEC-T1	Meisen CTCC	Cat# CTCC-400-0265; RRID: N/A

RESOURCE AVAILABILITY

Lead contact

Information and requests for resources should be directed to Dr. Xiao (yxerhazhishen@163.com).

Materials availability

This study did not generate new unique reagents.

Data and code availability

- This manuscript did not utilize or report original code.
- The original data for this manuscript is available.
- Any additional information required to reanalyze the data reported in this paper is available from the [lead contact](#) upon request.

EXPERIMENTAL MODEL AND STUDY PARTICIPANT DETAILS

Animal care ethics statement

Mice were used in strict accordance with the recommendations in the Guide for the Care and Use of the Laboratory Animals of the Nanjing Medical University and Approval obtained from the Animal Ethics Committee of Nanjing Medical University (Approval Code: 2111041, Approval Date: 17 November 2021). Mice were maintained under pathogen-free conditions in the animal facility and mice were sacrificed according to the Guide for the Care and Use of Laboratory Animals of Nanjing Medical University.

This study and publication of clinical data were approved by the Ethics Committee of Nanjing Medical University. Written informed consent was also signed by patients and their guardians. Animal experiments were also approved by the Animal Ethics Committee of Nanjing Medical University (Approval Code: 2111041, Approval Date: 17 November 2021).

METHOD DETAILS

Patients, tissues and follow-up

The clinical data and tissues of 80 patients with HCC confirmed by pathology were collected from January 2014 to February 2020 in the Department of Hepatobiliary Centre, the First Affiliated Hospital of Nanjing Medical University. All patients were treated with surgical procedures. They were followed up by telephone or outpatient review, and the follow-up period extended up to 31st February 2021. This study was approved by the institutional ethical review board, and written informed consent was signed by all patients and their guardians.

Cell lines and culture

HCC cell lines (Hep-3B, HCC-LM3) and HEK293T cells were purchased from Shanghai Institute of cell biology, Chinese Academy of Sciences (Shanghai, China). They were cultured in DMEM medium (Gibco BRL, Gaithersburg, MD, USA) supplemented with high glucose, 10% fetal bovine serum (FBS) (TransGen Biotech, Beijing, China) and 1% Penicillin-Streptomycin (TransGen Biotech, Beijing, China). HUVECs (PUMC-HUVEC-T1) were acquired from Chinese Academy of Sciences (Meisen CTCC, Zhejiang, China) and were grown in ECM specific medium (Meisen CTCC, Zhejiang, China). All the above cells were placed in a cell incubator containing 5% CO₂ at 37°C. Under normoxia, cells were cultured in a cell incubator containing 20% O₂ at 37°C. To simulate anoxic condition, the cells were cultured in a tri-gas incubator containing 5% O₂ at 37°C.

Isolation and identification of exosomes from HCC cells

HCC cells were cultured in complete medium containing 10% FBS without exosomes and the medium was collected after 48h. Modified ultracentrifugation was adopted to extract exosomes, following MISEV 2018 guidelines.³¹ The collected supernatant was first centrifuged at 500g for 10 min at 4°C to remove dead cells and then it was centrifuged again at 2000g for 20 min at 4°C to eliminate cell debris. The liquid was centrifuged at 10000g for 30 min at 4°C and filtered through a sieve with 0.22µm aperture to clear larger vesicles. Finally, the filtrate was ultracentrifuged twice at 110000g for 70 min at 4°C each time with an Optima XPN-100 Ultracentrifuge (Beckman Coulter, USA). The precipitates obtained from supernatant were resuspended with phosphate buffered saline (PBS) and stored at -80°C. The collected exosomes were observed under a FEI Tecnai G2 Spirit Bio TWIN transmission electron microscope (FEI, USA) and the abundance and particle size of exosomes were detected by a Zetasizer Ultra particle tracker (Malvern, UK).

Transfection and treatment of HCC-derived exosomes

Mimics and inhibitor of miR-3174 (RiboBio, Guangzhou, China) marked by Cy3 (red) were loaded into HCC-derived exosomes by a modified calcium chloride-mediated transfection method according to previous research of Zhang et al.³² Then these exosomes were labelled with PKH67 (green) dye liquid (Sigma-Aldrich, St. Louis MO, USA) and centrifuged again at 110000g for 70 min at 4°C to remove excess fluorescent dyes. Fluorescent labelled exosomes were incubated with HUVECs in dark at 37°C for 24h and the phagocytosis of exosomes by HUVECs was observed by a Stellaris STED laser confocal microscope (LEICA, Germany).

In previous study, we found that miR-3174 was expressed the highest in HCC-LM3 cells and the lowest in Hep-3B cells.¹² According to this, MiR-3174 mimics and mimic-NC (RiboBio, Guangzhou, China) as control were first loaded into exosomes derived from Hep-3B cells by above method. Then these exosomes containing miR-3174 mimics (Hep-3B/miR-3174-exo) or mimic-NC (Hep-3B/mock-exo) were co-cultured with HUVECs for 48h to construct miR-3174 overexpression models of HUVECs. MiR-3174 knockdown models of HUVECs were constructed by miR-3174 inhibitor (HCC-LM3/inhibitor-miR-3174-exo) and inhibitor-NC (HCC-LM3/NC-exo) as control in the same way. In the rescue assays, in order to inhibit the exosomes secreted by HCC cells, an inhibitor of exosomes named GW4869 (Sigma-Aldrich, St. Louis MO, USA) was added before these exosomes were isolated (Hep-3B/miR-3174-exo+GW4869). In the group of Hep-3B/miR-3174-exo+HIPK3, HUVECs were transfected with HIPK3 overexpression plasmids (CoreusBiotech, Nanjing, China) by Lipofectamine 3000 (Invitrogen, USA).

Scratch-healing assay

Scratching-healing assay was performed in 6-well culture plates (Corning, USA). When the confluence of HUVECs reached more than 95%, the scratch is simulated with the tip of 200ul pipette gun. After 72h, wound closure was observed and photographed under an inverted

microscope (ZEISS, Germany) and the percentage of closure area was measured and analyzed by Image J software. All experiments were performed in triplicate and each assay was repeated three times.

Transwell migration assay

250ul serum-free medium suspension containing HUVECs (4×10^4 cells/well) was added to each upper transwell chamber (8um pore size; Corning, USA) and 600ul medium with 20% FBS was poured into each lower chamber. After 24h, HUVECs in lower chambers were fixed with 4% paraformaldehyde, stained with 0.5% crystal violet for 30 minutes, washed and dried in turn. Finally, the lower chambers were photographed under a microscope and the numbers of migrated HUVECs were analyzed by Image J software. All experiments were performed in triplicate and each assay was repeated three times.

Tube formation assay

Tube formation assay was performed in 24-well culture plates. Before the experiment, the bottom of each well was covered with 200ul matrigel (BD, USA) and incubated for 30 min at 37°C. After the matrigel was solidified, 10×10^4 cells were seeded into each well and cultured for 12h. The number of rings formed by HUVECs in each group was calculated by Image J software. All experiments were performed in triplicate and each assay was repeated three times.

3D spheroid sprouting assay

The 3D spheroid sprouting assay was launched to evaluate the angiogenesis ability of HUVECs. Before the experiment, HUVECs (2000/well) were seeded into 96-well ultra-low adsorption culture plates with U-shaped bottom (Corning, USA) and cultured for 48h. During this period, HUVECs were treated under different conditions. After the spheroids were formed, they were centrifuged and resuspended in ECM medium with 20% methylcellulose for use. Then, type I collagen (Corning, USA), NaOH(1M) and ECM medium were mixed on ice in the ratio of 8:1:1 and the collagen solution was mixed with HUVEC spherical suspension in the ratio of 1:1.³³ Total 150ul/well solution was added into the 96-well culture plates and 150ul/well ECM medium was supplemented after collagen solidification. After HUVEC spheroids were embedded in collagen and cultured for 3 days, the numbers of sprouts were estimated by Image J software. All experiments were performed in triplicate and each assay was repeated three times.

In vitro HUVECs permeability assay

Total 5×10^4 cells/well were seeded on the top of transwell chambers (0.4um pore size; Corning, USA) in advance and co-cultured with HCC-derived exosomes for 3 days. When HUVECs completely covered the upper chambers, rhodamine B isothiocyanate-dextran (Sigma, USA) was added into them and 10ul medium in each lower chamber was collected every hour for fluorescence intensity detection at 590nm emission and 544 nm excitation by fluorometer (Biotek synergy H1; Biotek, USA). All experiments were performed in triplicate and each assay was repeated three times.

Aortic ring assay

The thoracic aortas obtained from 6-week-old Wild Type (WT) mice were cut into 0.5mm- long rings after removing their adventitias. The rings were embedded in 96-well plates coated with matrigel and incubated for 30 minutes at 37°C, then conditioned medium was added to each well. After 7 days, the numbers of sprouts formed by aortic rings were measured by Image J software. All experiments were performed in triplicate and each assay was repeated three times.

Animal disease models and in vivo vascular permeability assay

All relevant animal experiments were approved by the Animal Ethics Committee of Nanjing Medical University (Nanjing, China). In subcutaneous tumor transplantation experiment, 6-week-old BALB/c nude mice (n=24) obtained from the Animal Experiment Center of Nanjing Medical University (Nanjing, China) were randomly divided into 4 groups (each group, n=6) and they were injected subcutaneously with HCC-LM3 or Hep-3B cells (10^6 cells/100μl, 100μl/ mouse). Not only that, they were injected with HCC-derived exosomes (5ug/mouse) via tail vein every 3 days for 2 weeks. On the 35th day after inoculation, all nude mice were sacrificed and the tumors were separated, photographed, measured and weighted. For construction of lung metastasis models, all nude mice (n=20) were randomly divided into 4 groups (each group, n=5) and injected with Hep-3B or HCC-LM3 cells (10^6 cells/100μl, 100μl/ mouse) via tail vein. Simultaneously, they were injected with HCC-derived exosomes (5ug/mouse) via tail vein every 3 days for 4 weeks. On the 60th day after injection, all nude mice were injected with PKH-67 labelled exosomes (green) and rhodamine B isothiocyanate-dextran (red) via tail vein. After 3h, they were sacrificed and their lungs were perfused with PBS to eliminate excess dyes. In the rescue assays, HCC cells in Hep-3B/miR-3174-exo+GW4869 group were pretreated with GW4869. In Hep-3B/miR-3174-exo+HIPK3 group, miR-3174 mimics and overexpression HIPK3 plasmids were simultaneously loaded into exosomes by above method.¹⁴ The lung tissues were photographed and stained with immunofluorescence and haematoxylin & eosin (H&E).

Dual luciferase reporter assay

HEK293T cells seeded on 6-well plates were co-transfected with miR-1275 mimics or NC duplex (labelled with Renilla luciferase) and plasmids containing WT or mutant 3'-UTR of HIPK3 (labelled with firefly luciferase). After 48h, all cells were lysed and the fluorescence intensity was

measured by fluorometer according to the instruction of kit (Vazyme, Nanjing, China). All experiments were performed in triplicate and each assay was repeated three times.

Immunohistochemical and immunofluorescent staining

The tissues or samples were fixed with 4% paraformaldehyde and then they were embedded in paraffin for immunohistochemical staining or in Tissue-Tek OCT (Miles, USA) for immunofluorescent staining. Primary antibodies used in immunohistochemical staining assay contained anti-Ki67 (Abcam, UK) and anti-CD34 (Servicebio, Wuhan, China). Primary antibodies applied to immunohistochemical staining assay contained anti-VE-cadherin (Proteintech, Wuhan, China), anti-ZO-1 (Abcam, UK), anti-p53 (Abcam, UK), anti-HIPK3 (Abcam, UK) and anti-HNRNPA1 (ABclonal, Wuhan, China). Fluorescent labelled secondary antibodies (Proteintech, Wuhan, China) including red (594nm) and green (488nm) were also involved in immunohistochemical staining assay.

Co-Immunoprecipitation (CO-IP) assay

Co-Immunoprecipitation (CO-IP) assay was explored to verify the interaction between p53 and HIPK3. Before this assay, HUVECs were transfected with HIPK3 overexpressing plasmids labelled with flag. Primary antibodies anti-p53 (Abcam, UK) and anti-DDDDK tag (Abcam, UK) and nonspecific antibody anti-IgG (Abcam, UK) were prepared. This assay was performed according to the instructions of IP kit (Thermo-fisher, USA).

Chromatin immunoprecipitation (ChIP) assay

HCC-LM3 and Hep-3B cells were cultured under hypoxia (5% O₂) for 48h before Chromatin immunoprecipitation (ChIP) assay. Primary antibodies anti-HIF-1 α (Abcam, UK) and anti-IgG (Abcam, UK) were prepared in advance. This assay was performed under the guidance of the instructions of Pierce Agarose ChIP Kit (ThermoFisher, USA). Sequence of the promoter region of miR-3174 was isolated from immunoprecipitation (IP) and amplified by PCR. The binding of HIF-1 α and the promoter region of miR-3174 was finally verified by agarose gel electrophoresis and dual luciferase reporter assays. The specific primer sequences were listed as follows (Table S1).

RNA immunoprecipitation (RIP) assay

RNA immunoprecipitation (RIP) assay was performed to explore the combination of miR-3174 and HNRNPA1. This assay was implemented on the basis of instructions of Millipore Magna RIP RNA Binding Protein IP Kit (Millipore, MA, USA) and primary antibodies anti-HNRNPA1 and anti-IgG were also prepared. The expression levels of miR-3174 in each group were detected by qRT-PCR.

Quantitative real-time polymerase chain reaction (qRT-PCR)

Total RNAs were extracted from tissues or cells by centrifugal column method (Vazyme, Nanjing, China). The purity and concentration of RNAs were determined by Nanodrop 2000 microplate reader (ThermoFisher, USA). Reverse transcription was experimented by the HiScript II QRT SuperMix for qPCR (Vazyme, Nanjing, China). Quantitative real-time polymerase chain reaction (qRT-PCR) was implemented by ChamQ Universal SYBR qPCR Master Mix (Vazyme, Nanjing, China) and 7900HT Fast Real-Time PCR System (ABI, USA). The primer sequences were listed as follows (Table S1).

Western blot (WB) analysis

The specific primary antibodies involved in western blot (WB) analysis were as follows: anti-VE-cadherin (1:1000), anti-ZO-1 (1:1000), anti-TSG101 (1:1000, Abcam, UK), anti-VEGFR-2 (1:1000, Abcam, UK), anti-Fas (1:1000, Abcam, UK), anti-p53 (1:1000), anti-HIPK3 (1:1000), anti-Caspase-3 (1:1000, Abcam, UK), anti-HNRNPA1 (1:1000), anti-HIF-1 α (1:1000), anti-DDDDK tag (1:1000), anti-CD9 (1:1000, Abcam, UK), anti-CD63 (1:1000, Abcam, UK), anti-ALIX (1:1000, Abcam, UK), anti- β -actin (1:1000, Proteintech, Wuhan, China), anti-SFRS2 (1:1000, Abcam, UK), anti-ACO-1 (1:1000, Abcam, UK). The secondary antibody was HRP-IgG (1:10000, Proteintech, Wuhan, China) and β -actin was used as internal reference.

Bioinformatics analysis and online public databases

Several online public databases related to transcriptome RNA sequencing data and clinical information of HCC samples from TCGA database were applied to predict the functions and prognosis of miR-3174, HNRNPA1 and HIPK3, including StarBase (<https://starbase.sysu.edu.cn/>), CancerMIRNome (<http://bioinfo.jialab-ucr.org/CancerMIRNome/>), GEPIA (<http://gepia.cancer-pku.cn/>), Timer (cistrome.shinyapps.io/timer), Kaplan-Meier Plotter (<http://kmplot.com/analysis/>) and Human Protein Atlas (<https://www.proteinatlas.org/>). Four databases (TargetScan, miRWalk, miRDB and miRPathDB) were used to predict target genes of miR-3174 and RBPDB (<http://rbpdb.ccb.utoronto.ca/>) was involved in exploring the binding site of miR-3174 and HNRNPA1. PanglaoDB single cell database (<https://panglaoDB.se/index.html>) was applied to predict cells that can specifically express HIPK3. The abundances of interstitial cells in HCC tissues based on TCGA-LIHC database was measured by Microenvironment Cell Populations-counter (MCP-counter) algorithm via R software (version 4.1.0). The databases named JASPAR (<https://jaspar.genereg.net/>) and mirTrans (<http://mcube.nju.edu.cn/jwang/lab/soft/mirtrans/>) were applied to forecast the transcription regulators of miR-3174. The protein database STRING (<http://string-db.org/>) was in use on predicting the interaction

between p53 and HIPK3. Molecular docking was performed to simulate the combination of HIPK3 and p53 on HSYMDOCK Server (<http://huanglab.phys.hust.edu.cn/hsymdock/>).

QUANTIFICATION AND STATISTICAL ANALYSIS

All data were collected from at least three independent assays. The means and standard deviations were exhibited in curve graphs. The Chi-squared test and Student's *t* test were applied to evaluate the significance of differences between groups. The experimental data were analyzed by Graphpad prism 8.0 software. Clinical data and cox proportional-hazards model analysis were performed by SPSS 22.0 software. Pearson's correlation test was used for correlation analysis and Statistically significance was defined as $p < 0.05$ (*), $p < 0.01$ (**), and $p < 0.001$ (***)